Nanoscale Advances

ROYAL SOCIETY OF CHEMISTRY

REVIEW

View Article Online
View Journal | View Issue

Cite this: *Nanoscale Adv.*, 2021, **3**, 2975

Tumor-targeting inorganic nanomaterials synthesized by living cells

Yuzhu Yao, [a] Dongdong Wang, [a] Jun Hu *[abc] and Xiangliang Yang *[abc]

Inorganic nanomaterials (NMs) have shown potential application in tumor-targeting theranostics, owing to their unique physicochemical properties. Some living cells in nature can absorb surrounding ions in the environment and then convert them into nanomaterials after a series of intracellular/extracellular biochemical reactions. Inspired by that, a variety of living cells have been used as biofactories to produce metallic/metallic alloy NMs, metalloid NMs, oxide NMs and chalcogenide NMs, which are usually automatically capped with biomolecules originating from the living cells, benefitting their tumor-targeting applications. In this review, we summarize the biosynthesis of inorganic nanomaterials in different types of living cells including bacteria, fungi, plant cells and animal cells, accompanied by their application in tumor-targeting theranostics. The mechanisms involving inorganic-ion bioreduction and detoxification as well as biomineralization are emphasized. Based on the mechanisms, we describe the size and morphology control of the products *via* the modulation of precursor ion concentration, pH, temperature, and incubation time, as well as cell metabolism by a genetic engineering strategy. The strengths and weaknesses of these biosynthetic processes are compared in terms of the controllability, scalability and cooperativity during applications. Future research in this area will add to the diversity of available inorganic nanomaterials as well as their quality and biosafety.

Received 28th February 2021
Accepted 5th April 2021

DOI: 10.1039/d1na00155h

rsc.li/nanoscale-advances

Introduction

With the development of nanotechnology, inorganic nanomaterials are widely produced and applied in the biomedical field, as detection, diagnostic, monitoring, and therapeutic tools.[1–5] However, inorganic nanomaterials synthesized by conventional methods (such as hydrothermal or solvothermal methods) are far from satisfactory due to their poor biocompatibility, poor targeting effect, and low bioavailability. Inspired by the biosynthesis process in nature, inorganic nanomaterials

[a]*National Engineering Research Center for Nanomedicine, College of Life Science and Technology, Huazhong University of Science and Technology, Wuhan 430074, China*
[b]*Hubei Key Laboratory of Bioinorganic Chemistry and Materia Medica, School of Chemistry and Chemical Engineering, Huazhong University of Science and Technology, Wuhan 430074, China*
[c]*Key Laboratory of Molecular Biophysics of Ministry of Education, College of Life Science and Technology, Huazhong University of Science and Technology, Wuhan 430074, China. E-mail: hjun0718@hust.edu.cn; yangxl@hust.edu.cn*

Yuzhu Yao received her Bachelor's degree from Huazhong University of Science and Technology (HUST) in 2015. She is now studying as a PhD candidate under the guidance of Dr Jun Hu and Prof. Xiangliang Yang. Her current research interest is biosynthetic nanomaterials for tumor theranostics.

Dongdong Wang is studying for a PhD in Huazhong University of Science and Technology (HUST), and received his Master's degree from Lanzhou University. His research interest is the application of biomimetic nano drug delivery systems in tumor targeted therapy.

based on living cell synthesis have attracted researchers' attention.

The synthesis of inorganic materials by living cells is widespread in nature. For example, orientationally arranged magnetic nanoparticles (NPs) can be fabricated within magnetotactic bacteria to make them susceptible to the geomagnetic field, which helps them to swim to deep water with relatively low oxygen content.[6] Some living plants and microalgae can absorb metal ions in water or soil and then convert them to insoluble nanomaterials to mitigate environmental stress.[7,8] Inspired by nature, a variety of inorganic nanomaterials (NMs) including metallic/metallic alloy NMs, metalloid NMs, oxide NMs and chalcogenide NMs could be constructed intracellularly or extracellularly by living cells of bacteria, fungi, animals and plants. For example, Kangpeng Wang *et al.* reported the biosynthesis of Te nanostructures by growing *Bacillus selenitireducens* in a lactate-tellurite medium.[9] Qing-Ying Luo *et al.* employed yeast cells to synthesize CdSe quantum dots (QDs) intracellularly.[10] Maonan Wang reported the *in situ* biosynthesis of Au nanoclusters (NCs) using both cultured cancer cells and tumors of an orthotropic liver tumor mouse model.[11] Alejandra Arévalo-Gallegos *et al.* used *Botryococcus braunii* as a bioreactor for the production of Ag nanoparticles.[12]

Living cell synthesis can be conducted at room temperature with less energy consumption and negligible hazardous waste generation, and the obtained biosynthetic nanomaterials have the characteristics of good biocompatibility and unique biological properties. The ever-growing interest and significant progress of biosynthetic nanomaterials have witnessed broad prospects in biomedical applications due to their combined advantages of natural substances and nanotechnology.[13] For example, engineered bacteria with photothermally controlled TNF-α expression and Au nanoparticles synthesized intracellularly along with near-infrared (NIR) realized efficient tumor-targeting therapy due to their preference for hypoxic and nutrient-rich regions.[14] *In situ* biosynthesized Au NCs in tumor cells were proved to suppress cancer development *via* the inhibition of the P13K-AKT signalling pathway.[15]

However, compared with chemical synthesis processes, the size and morphology of the synthesized nanomaterials by living cells are usually uncontrollable. As we all know, both the size and morphology have crucial impacts on the properties of nanoparticles. They can be regulated to a certain extent through pH, temperature, precursor type and proportion, and incubation time, such as the pH-controlled morphology of Au nanoparticles synthesized by living plants,[16] temperature-adjusted fluorescence intensity of CdSe QDs synthesized by fungus *F. oxysporum*,[17] and incubation time-regulated size and emission wavelength of CdTe QDs synthesized by bacteria.[18] But these simple adjustments are far from satisfactory. For the higher controllability of biosynthetic processes, the mechanism of the formation of inorganic nanomaterials within different types of living cells should be clarified first. Bioreduction and detoxification as well as biomineralization are often involved in the mechanism of biosynthesis. Many kinds of intracellular enzymes, reducing molecules such as glutathione and glucose, cell surface expressed polysaccharides and proteins *etc.* usually participate in these complicated reactions.[19–21] By adjusting the expression level of target proteins or peptides by means of genetic engineering, the metabolic pathway, redox state *etc.* of living cells can be regulated, so as to regulate the composition, morphology, size and yield of synthesized nanomaterials. For instance, the recombinant *Escherichia coli* (*E. coli*) coexpressing metallothionein (MT) and phytochelatin synthase (PCS) showed enhanced metal binding capacity and promoted the assembly of diverse metal elements into highly ordered NPs.[22] The yield of CdSe QDs was significantly improved by impairing the extracellular electron transfer (EET) ability of the bacteria *via* the deletion of the CymA-encoding gene.[23]

In general, biosynthesis using living cells has emerged as an innovative and attractive green chemical methodology for the preparation of inorganic nanomaterials. In this review, we summarize the biosynthesis of inorganic nanomaterials in different types of living cells including bacteria, fungi, plant cells, and animal cells, while the strengths and weaknesses of the biosynthetic processes are systematically presented,

Dr Jun Hu is an associate professor in the College of Life Science and Technology, Huazhong University of Science and Technology. He earned his PhD degree in 2011 from the College of Chemistry and Molecular Science at Wuhan University. His research is focused on the biomedical applications of multifunctional inorganic nanomaterials in the field of tumor diagnosis and therapy.

Dr Xiangliang Yang obtained his PhD degree from Huazhong University of Science and Technology in 1995. He is currently a full professor in the College of Life Science and Technology, Huazhong University of Science and Technology. He serves as the Director of the National Engineering Research Center for Nanomedicine. He is a panel member of the National Key Research and Development Plan "Nano Science & Technology" Key Project. His research focuses on nanomedicine, including nanodrug delivery systems, nanodiagnostics and biomedical nanomaterials.

especially for application in tumor-targeting theranostics (Scheme 1). The mechanisms of the biosynthesis are analysed and it is generally accepted that inorganic-ion bioreduction and detoxification as well as biomineralization are usually involved. For controlling the size and morphology of the products, the modulation of precursor ion concentration, pH, temperature, and incubation time, as well as cell metabolism by a genetic engineering strategy is proposed in many cases. However, from the perspective of biomedical application, there are still some issues that need to be addressed which are indicated in the last part of the review. Future research in this area will add to the diversity of available inorganic nanomaterials as well as their quality and biosafety.

Bacterial synthesis

Bacteria, a kind of unicellular prokaryote, have been widely studied in living-cell biosynthesis of inorganic nanomaterials[23–25] owing to their characteristics of single cell growth, facile cultivation, rapid proliferation, and easy genetic manipulation.[26] Metal ions and some oxyanions can be taken up by bacteria to participate in their metabolic processes to produce metallic/metalloid NMs, oxide NMs and chalcogenide NMs through biomineralization, bioreduction or intracellular detoxification.

Metal oxide NMs synthesized through biomineralization

The most famous case of bacterial synthesis is magnetic nanoparticles intracellularly formed by magnetotactic bacteria. In 1975, R. Blackmore for the first time observed and reported the magnetotactic bacteria (MTB), which could swim aligned parallel to the Earth's geomagnetic field.[27] The MTB were found to naturally synthesize intracellular chains of magnetic nanoparticles (called magnetosomes), with a structure of one magnetic mineral nanocrystal core and surrounding phospholipids and proteins (Fig. 1A).[28–30] The magnetosome biogenesis has been shown to consist of the formation of an empty magnetosome membrane through the invagination of the cytoplasmic membrane, magnetosome protein sorting to the magnetosome membrane, iron transportation into the magnetosome membrane and biomineralization as iron-rich magnetic nanocrystals, and the final assembly and positioning of the

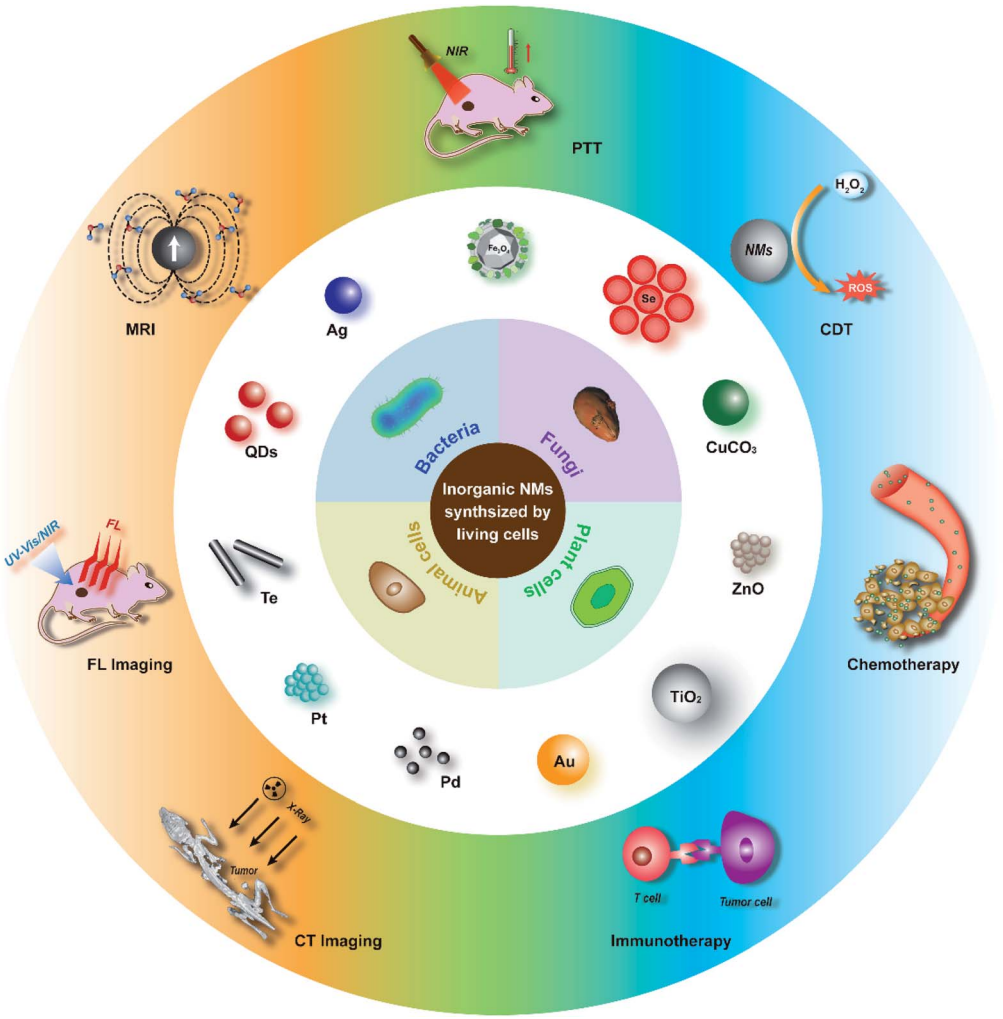

Scheme 1 Inorganic nanomaterials synthesized by living cells for tumor-targeting theranostics.

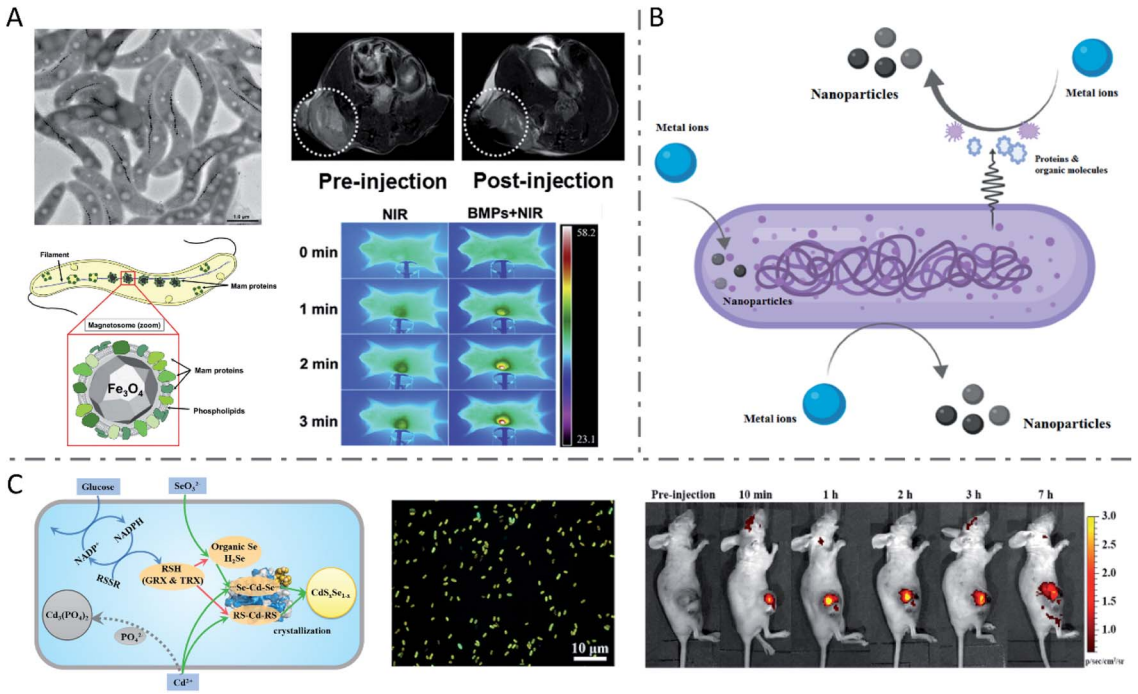

Fig. 1 Inorganic nanoparticles synthesized by wild-type bacteria. (A) Biosynthesis of magnetosomes by MTB and application in T2 weighted MRI and PTT of tumors. Reproduced from ref. 28 with permission from American Society for Microbiology, copyright 2019. Reproduced from ref. 34 with permission from Elsevier Ltd., copyright 2016. (B) Biosynthesis mechanism of metal nanoparticles by bacteria. Reproduced from ref. 44 with permission from American Chemical Society, copyright 2020. (C) Metabolism-regulated Se and Cd biotransformation pathways in *E. coli*, and *in vitro* and *in vivo* fluorescence images of the synthesized QDs in glucose-facilitated *E. coli* cells. Reproduced from ref. 26 with permission from American Chemical Society, copyright 2019.

magnetosome chain.[31] In studies to reveal the mechanism of magnetosome synthesis, researchers found that the protein MamP had unique protein-folding structures called magnetochrome domains which contributed to the attraction for iron.[32] MamP can oxidize Fe(II) to Fe(III), and eventually synthesize Fe_3O_4 containing both Fe(II) and Fe(III). It was verified *in vitro* that Fe(II) was finally transformed to Fe(III) in the presence of MamP Fe(II). Due to the inherent hypoxia-targeting and magnetic-targeting ability of the MTB and the magnetic and thermal properties of magnetosomes,[33] the MTB have been widely used in enhanced magnetic resonance imaging (MRI),[34] fluorescence imaging and probing,[35–37] as well as tumor-targeting magnetic hyperthermal therapy (MHT)[38] and photothermal therapy (PTT).[39] Chuanfang Chen *et al.* reported that the bacterial magnetic nanoparticles (BMPs) isolated from the MTB successfully achieved T2-weighted MRI enhancement and PTT of tumors (Fig. 1A).[34]

Metallic NMs synthesized through detoxification

Inspired by the naturally biosynthesized nanomaterials, a variety of bacteria have been explored as biofactories to synthesize a diverse range of nanomaterials. Different from Fe ions, noble metal ions in the environment are usually toxic to bacteria. To mitigate environmental stress, they are commonly reduced to their insoluble form by the bioactive molecules or proteins present inside bacteria (such as nicotinamide dinucleotide (NADH),[40] reduced nicotinamide dinucleotide phosphate (NADPH),[26,41] glutathione (GSH),[41,42] glutathione reductase (GR),[41] nitrate reductase (NR),[14] fumarate reductase FccA,[43] *etc.*), as well as by the cell surface expressed or extracellularly secreted reducing species (Fig. 1B).[44] Bioreduction[45,46] or intracellular detoxification[18,47] is often involved in this process.

Various functional groups including thiol, carboxyl, and amino groups present on the surface of bacteria have high affinity for metal ions. Upon reduction with reducing species originating from bacteria or extra added ones, metallic NMs are formed through nucleation and surface growth. For example, *E. coli* was used as a biofactory to reduce chloroauric acid and modulate the formation of Au NPs on the bacterial surface, in which sugars or enzymes might modulate the biosynthesis.[48] Gary Attard *et al.* demonstrated the synthesis of Pt NPs by *E. coli* MC4100 with different degrees of metal loading, in which Pt(II) bound on the surface of bacteria was reduced to Pt(0) by sparging hydrogen into the suspension.[49] In a recent study, bimetallic Au–Ag nanoparticles were biosynthesized by *E. coli*, in which Au ions were reduced by the phenolic group of tyrosine residues present in the surface protein of *E. coli*.[50] At basic pH, the phenolic group converted into a negative phenolic ion that can reduce Au ions to Au atoms.[51] After the formation of Au NPs, an Au–Ag core–shell nanostructure was obtained with the combination of Ag ions. Compared with single Au or Ag nanoparticles, the biosynthesized Au–Ag bimetallic NPs showed enhanced photothermal therapy performance and antibacterial ability.

Under environmental stress, heavy metal ions can be intracellularly accumulated by bacteria through the transport system and then converted into insoluble zero-valent nanoparticles, such as Au NPs,[52] Ag NPs,[52,53] and Cu NPs.[54] For example, Au, Ag and Au–Ag alloy crystals were synthesized by *Lactobacillus* strains *via* incubation with the corresponding precursor ions.[52] The bacteria with crystals synthesized remained viable, and the coalescence of the nanoclusters was considered to be protective for the living cells by reducing the surface area of the crystals. In another study, an *E. coli* strain that carried chromosomally encoded silver resistance determinants was observed to form Ag NPs in the periplasmic space upon exposure to Ag^+ ions.[53]

Metalloid NMs synthesized through bioreduction

Different from the metal detoxification mechanism, for some elements such as Se and Te, their oxyanions could participate in the respiratory chain process as respiratory electron acceptors, and finally could be reduced to a low-valent state. Anaerobic bacterium *Bacillus selenitireducens* was used to synthesize Te nanostructures at room temperature.[9] In another study, intracellular synthesis of Te nanorods (NRs) by living *Staphylococcus aureus* (*S. aureus*) cells *via* intracellular reduction of TeO_3^{2-} was reported, and the intracellular biochemical pathways were studied.[41] The Te(IV) in TeO_3^{2-} was first reduced to GSTeSG by intracellular GSH, and further reduced to GSTeH by NADPH and GR. The resulting intermediate GSTeH spontaneously decomposed into Te(0), and finally formed Te nanorods. To verify this mechanism, *in vitro* synthesis of high-quality Te nanorods was successfully achieved using a quasi-biological system containing electrolytes, reduced GSH, reduced NADPH and GR, which were involved in the intracellular reaction. It was further verified that the length of TeNRs can be adjusted both by changing the concentration of NaOH to control the concentration of Te(0) and by changing the concentration of GR to control the generation rate of Te(0). Considering the great photothermal conversion ability of Te[55–57] and the tumor-targeting ability and immune response activation of bacteria,[58–61] our recent work (unpublished) employed bacteria with Te nanorods synthesized intracellularly as a comprehensive treatment system in tumor-targeting photothermal immunotherapy. Belonging to the same family within the periodic table as Te, Se in Na_2SeO_3 could also be reduced to low-valence Se by certain bacteria.[43,62] *Shewanella oneidensis* (*S. oneidensis*) MR-1, a model dissimilatory metal-reducing bacterium (DMRB), can respire on multiple metal ions to produce nanoparticles through dissimilatory respiration and energy derivation.[43,63,64] Dao-Bo Li *et al.* reported that fumarate reductase FccA is the terminal reductase of selenite in the periplasm of *S. oneidensis*, and c-type cytochrome CymA, which is central to respiration, is of vital importance in the reduction process.[43]

Metallic chalcogenides synthesized by bacteria

Combining the two processes mentioned above, a number of metallic chalcogenides can be synthesized by living bacteria, among which the most representative ones are QDs. Quantum dots are a kind of inorganic semiconductor nanocrystal with excellent optical properties, such as tunable emission with size and components in a wide spectral range, high photo stability and fluorescence quantum yield, and a long fluorescence life time, which endow them with great potential in bio-labelling and detection, *in vivo* imaging and tracking, and tumor-targeting drug delivery and therapy.[65–69] Zhang Yi *et al.* prepared CdSe/CdS QDs with good water solubility and distinct yellow fluorescence using *E. coli* cells for *in vitro* Hg^{2+} detection.[70] It was reported that glucose addition to the culture medium of *E. coli* would change the metabolic route of the Se and Cd from $Cd(PO_4)_2$ formation to CdS_xSe_{1-x} QDs assembly, yielding fluorescent bio-QDs (Fig. 1C).[26] The researchers presented that glucose metabolism improved the NADPH production, thus leading to more reduced thiol groups (RSH), which were critically responsible for Se reduction and Cd binding, thereby significantly raising the CdS_xSe_{1-x} QDs synthesis rate and yield. The resulting QDs were successfully applied for imaging tumors. Moreover, *S. aureus* cells were also used to synthesize $CdS_{0.5}Se_{0.5}$ QDs with outstanding photostability and high luminance through the "space–time coupling strategy".[47] By adding Na_2SeO_3 and $CdCl_2$ to *S. aureus* suspension at different times, the Cd precursor formed by Cd^{2+} detoxification can react precisely with the low-valence organoselenium compounds resulting from intracellular GR-involved Na_2SeO_3 reduction, to create $CdS_{0.5}Se_{0.5}$ *in vivo*, which can never occur in living cells in nature. Due to the specific interaction between the protein A expressed on the *S. aureus* surface and the Fc fragment domain of antibodies, the constructed cellular beacons (fluorescent cells) can be easily and widely applied as nanobioprobes for pathogen detection *in vitro*. Another study constructed a system for *in vitro* detection of human prostate-specific antigens using biosynthesized QDs in a similar way as above.[71] Haifeng Bao *et al.* reported the extracellular biosynthesis of CdTe QDs by *E. coli*, directly based on secreted proteins.[18] It was found that the size of bacteria-synthesized CdTe QDs increased with prolonged incubation time, with a red shift of the absorption edge and emission peak. The obtained QDs with size-tunable optical properties were functionalized with folic acid and employed to image cancer cells *in vitro*.

Engineered bacteria for biosynthesis

Although many species of bacteria can be used to synthesize inorganic nanomaterials, the types of nanomaterials prepared by wild-type (WT) bacteria are still limited, and their size and morphology are often uncontrollable. However, size and morphology have a crucial influence on the properties of nanomaterials. Therefore, genetically engineered bacteria have been used for more extensive and more controlled synthesis of nanomaterials, which is the most significant advantage of bacteria over other living cells. *E. coli* is one of the widely studied bacterial species for nanomaterial biosynthesis, with finely controllable genomic and metabolic functions.[72–75] After being engineered to express MT and/or PCS, recombinant *E. coli*

cells were incubated with various metal ions, including semiconducting (Cd, Se, Zn, Te), alkali-earth (Cs, Sr), magnetic (Fe, Co, Ni, Mn), and noble (Au, Ag) metals and rare-earth fluorides (Pr, Gd), to synthesize the corresponding metal NPs.[21] In the synthesis processes, MTs are capable of binding heavy metals (*i.e.*, Cu, Cd, and Zn), while the metal-binding peptide phytochelatin (PC) synthesized by PCS plays a significant role in heavy-metal detoxification processes, as a family of cysteine-rich, thiol-reactive peptides that bind several toxic metals (*i.e.*, Cu, Zn, Cd, Hg, and Pb). Thus, the engineering of *E. coli* led to the enhanced assembly of diverse metal elements into highly ordered NPs. This was the first time that an engineered bacterium was used for *in vivo* synthesis of a wide range of functional metal NPs. In the same study, it was demonstrated that the synthesized inorganic nanomaterials after feeding different concentrations of precursor metal ions exhibited various diameters, which further manifested as diverse colors and fluorescence emission wavelengths of QDs. The engineered *E. coli* cells were also employed to synthesize FeCo nanoparticles, the diameter of which could be tuned from (3.02 ± 1.00) to (5.57 ± 1.04) nm by varying the concentration of Fe^{2+} (or Fe^{4+}) and Co^{2+} ions from 0.5 to 2.0 mM. Subsequently, Yoojin Choi *et al.* scanned the periodic table to select 35 elements and biosynthesized 60 different nanomaterials by employing a recombinant *E. coli* strain coexpressing MT and PCS (Fig. 2A).[40] For most nanomaterials in the study, the biosynthesis begins in the cytoplasm, where MT and PC exist, and then the nanomaterials move to the cell wall to continue the synthesis. Moreover, the metal ions nucleate with PCs as a binding template and nucleation site, and are stabilized by PCs to prevent further aggregation. A Pourbaix diagram that summarized the producibility and crystallinity of a series of synthesized nanomaterials was used to predict the suitable reduction potential (Eh) and pH for nanomaterial biosynthesis. Then, through shifting the initial pH of *in vivo* reactions from 6.5 to 7.5, various crystalline nanomaterials of previously amorphous or not-synthesized ones were successfully synthesized by living cells of *E. coli* coexpressing MT and PCS. With respect to QDs, a study on *S. oneidensis* MR-1 showed that abundant Se and a small amount of CdSe nanoparticles were observed in WT bacterial cells after exposure to Na_2SeO_3 and $CdCl_2$ (Fig. 2B).[23] Then, *S. oneidensis* mutants with the CymA-encoding gene deleted (Δ*cym*A) or overexpressed (P_{YYDT}-*cym*A) were constructed to impair or promote the intrinsic EET ability. The Δ*cym*A showed high production of CdSe and low production of Se nanoparticles, while the P_{YYDT}-*cym*A performed oppositely.

Applications in tumor-targeting theranostics

Since numerous bacterial strains have an innate ability to target tumors due to their preference for hypoxic and nutrient-rich regions, nanomaterials synthesized in bacterial cells could be delivered to tumors directly with bacteria as carriers.[76–79] Moreover, outer membrane proteins expressed on the surface of bacteria could interact with antigen-presenting cells to elicit an immune response to synergize with the nanomaterials to enhance their therapeutic effect.[80,81] Additionally, outer membrane proteins can also serve as templates to realize the biomineralization of nanomaterials on the surface of bacteria, retaining the excellent tumor-targeting ability and immunogenicity of bacteria. For example, thermally sensitive programmable bacteria (TPB) expressing therapeutic proteins TNF-α were employed to synthesize Au nanoparticles *via* electron shuttle enzymatic metal reduction, to obtain TPB@Au.[14] The constructed bacteria-based antitumor vehicles along with NIR achieved satisfactory tumor-targeting therapeutic efficiency *via* oral administration.[14] In another study, Pd nanoparticles were biomineralized by *S. oneidensis* MR-1 on its surface to form the so-called "photothermal bacterium" (PTB).[64] The living PTB was further modified with zeolitic imidazole framework-90 (ZIF-90) encapsulating photosensitizer methylene blue (MB), which

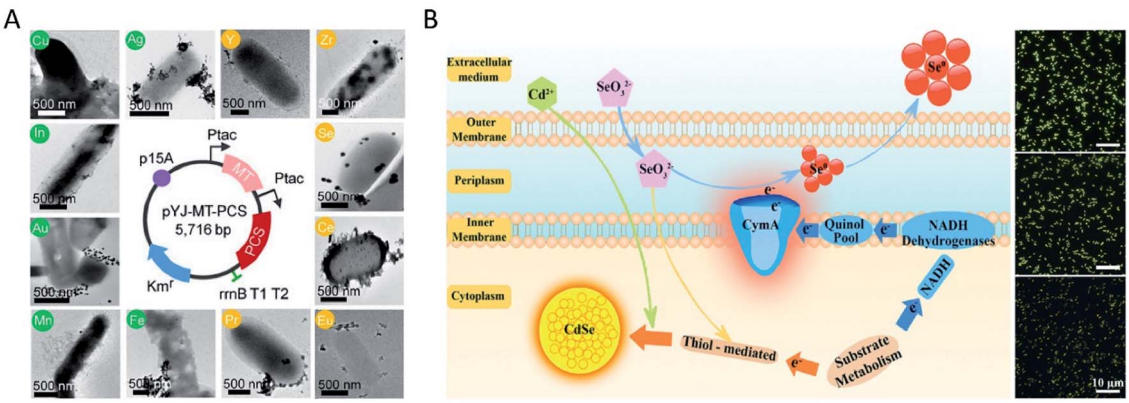

Fig. 2 Inorganic nanoparticles synthesized by engineered bacteria. (A) The map of plasmid pYJ-MT-PCS used to construct the recombinant *E. coli* DH5α strain coexpressing MT and PCS, and TEM images of nanomaterials synthesized *in vivo* with their corresponding elements labeled in circles. Reproduced from ref. 40 with permission from the National Academy of Sciences, copyright 2018. (B) Schematic diagram of the EET-dependent synthesis of nanoparticles by *S. oneidensis* MR-1, and fluorescence microscopy images of the biosynthesized nanomaterials *in vivo* by Δ*cym*A (above), WT (middle) and P_{YYDT}-*cym*A (below). Reproduced from ref. 23 with permission from American Chemical Society, copyright 2017.

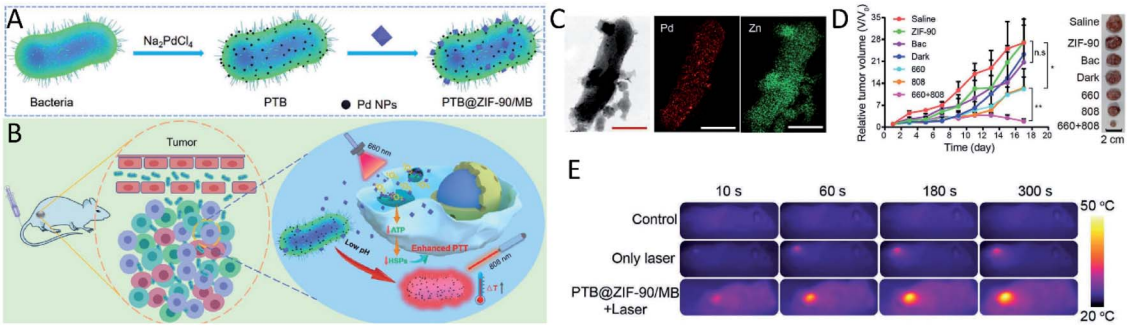

Fig. 3 Bacteria with inorganic nanomaterials synthesized on their surface for tumor-targeting therapy. Schematic illustration of the (A) synthetic procedure of PTB and PTB@ZIF-90/MB and (B) application in tumor-targeting PTT. (C) TEM-assisted element mapping of Pd and Zn on PTB@ZIF-90/MB (scale bar: 500 nm). (D) The antitumor efficiency and (E) photothermal property study of PTB@ZIF-90/MB in mice. Reproduced from ref. 64 with permission from WILEY-VCH Verlag GmbH & Co. KGaA, Weinheim, copyright 2020.

can selectively release MB in mitochondria. The PTB@ZIF-90/MB showed a significant tumor PTT effect, due to the selective targeting and tumor heat resistance suppression (Fig. 3).

In addition to these mentioned above, some other inorganic nanomaterials such as MnO_x nanospindles can be synthesized extracellularly by *E. coli* to encapsulate the chemotherapeutic agent doxorubicin (DOX) for tumor microenvironment responsive T1-weighted MRI enhancement and chemo-chemodynamic therapy.[46] These biosynthetic nanomaterials often show high colloidal stability, owing to the coating of biomolecules. Although WT bacteria have been successfully employed for the synthesis of several types of nanomaterials composed of noble metals, oxides and chalcogenides by using their inherent bioreduction or detoxification processes, the diversity as well as the size and composition of nanomaterials need to be better controlled. Biogenetic engineering seems to be an alternative strategy to address this issue. The production of nanomaterials by bacteria depends on their ability to resist the effects of environmental stress such as toxicity arising from metallic ions.[82] High concentration of toxic ions will induce the death of bacteria. Therefore, the efficiency of nanomaterial synthesis by bacteria is always low. Additionally, in terms of biomedical applications, the potential biological toxicity brought by bacteria especially pathogenic bacteria should be considered.[83]

Fungal synthesis

Fungi, a group of unicellular, multicellular, or syncytial spore-producing eukaryotic organisms, include yeasts, molds, mushrooms, *etc.*[84–86] Similar to bacteria, fungi have the advantages of significant growth rate, simple culture procedures, and facile and economical biomass handling for biosynthesis of nanomaterials.[87,88] Furthermore, fungi could tolerate higher metal concentrations, and secrete more extracellular enzymes and proteins than other microorganisms, thus leading to higher productivity of nanomaterials.[89–91] However, investigations on fungal synthesis are fewer than those on bacterial synthesis, mainly due to the fact that their structure makes it complicated to characterize the internal nanomaterials for microscopic and mechanistic studies.[92]

Synthesis by yeast cells

Yeasts, a family of various single-celled fungi that reproduce asexually by budding or division, have been broadly used in biosynthesis owing to their rapid proliferation and easy genetic manipulation.[93] Due to their strong ability to chelate toxic metals such as Cd, yeasts were extensively utilized for biosynthesis of QDs such as CdS,[94] CdSe,[10,19,95,96] and CdTe.[97] It was first reported in 1989 that CdS crystallites were obtained by incubating the yeasts *Candida glabrata* and *Schizosaccharomyces pombe* with cadmium salts.[94] When exposed to cadmium ions, the yeast cells produced metal-chelating peptides with a general structure of γ-$(Glu\text{-}Cys)_n$-Gly, which in turn bound with cadmium ions and controlled the nucleation and growth of CdS crystallites. Another metal sulphide nanocrystallite, *i.e.*, PbS, synthesized by yeast was reported in 2002.[98] Compared with CdS QDs, CdSe or CdTe QDs usually exhibited more excellent optical properties. Through complex intracellular biochemical reactions, Na_2SeO_3 or Na_2TeO_3 internalized by yeast cells can be metabolized to low-valence –SeH/–TeH in the cytoplasm. By the detoxification process, Cd^{2+} can be transformed to more stable $[Cd(GS)_2]^{2+}$ and eventually stored in the vacuoles of yeast cells. –SeH/–TeH and $[Cd(GS)_2]^{2+}$ are actually the precursors for the synthesis of CdSe or CdTe QDs. However, these two reactions are independent of each other in yeast cells. Thus, in order to obtain CdSe or CdTe QDs, it is a key point to make these two unrelated reactions sequentially occur at an appropriate time and space as desired. To address this issue, Ran Cui *et al.* proposed a "space–time coupling strategy" to synthesize CdSe QDs in living cells of *Saccharomyces cerevisiae* by feeding the cells with Na_2SeO_3 and $CdCl_2$ sequentially to collaboratively couple the intracellular metabolism of Na_2SeO_3 and detoxification of $CdCl_2$ (Fig. 4A).[96] Besides, by adjusting the incubation duration of the seleniumized yeast cells with $CdCl_2$ from 10 to 40 hours, CdSe QDs were obtained with tunable emission from green to yellow, then to red, and sizes from 2.69 to 6.34 nm. Se(IV) in SeO_3^{2-} was first reduced into the selenotrisulfide derivative of glutathione (GSSeSG) in the presence of reduced GSH, and further reduced into low-valence organoselenium compounds by GSH-related enzymes (NADPH and GR), in the cytoplasm and mitochondria of yeast cells. Then, the $Cd(SG)_2$

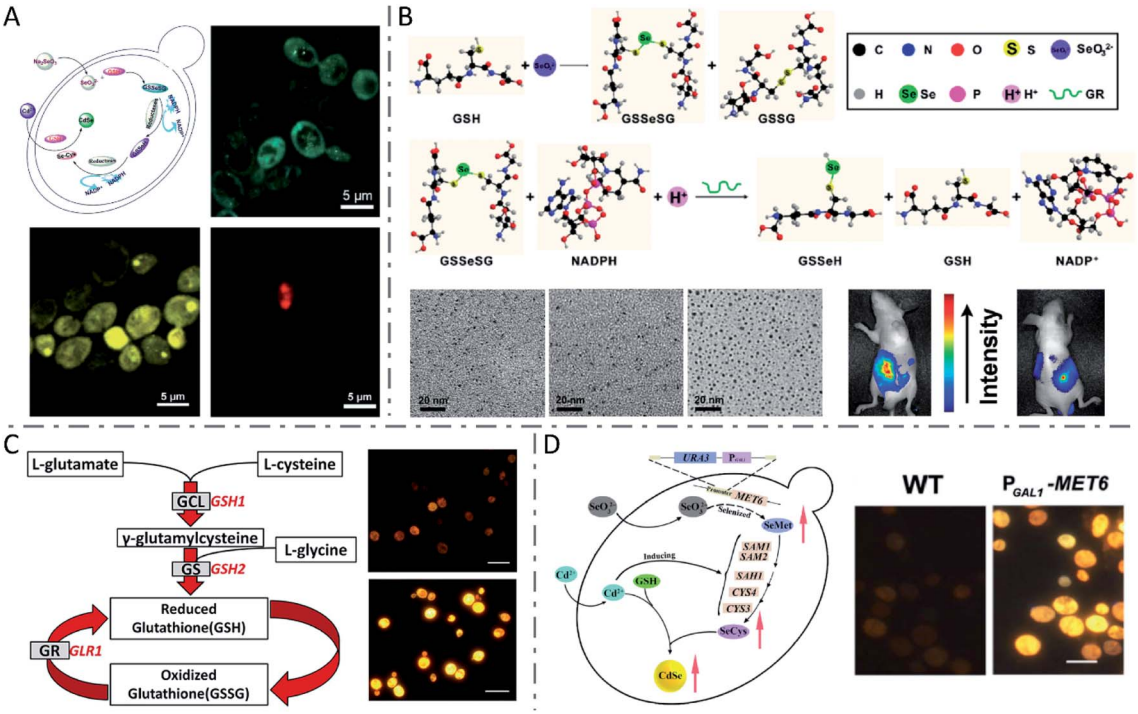

Fig. 4 QDs synthesized by yeast cells and the quasi-biosystem. (A) Route for unnatural biosynthesis of fluorescent CdSe QDs, and fluorescence microscopy images of seleniumized yeast cells cultured with $CdCl_2$ for 12 h (green), 24 h (yellow) and 40 h (red). Reproduced from ref. 96 with permission from WILEY-VCH Verlag GmbH & Co. KGaA, Weinheim, copyright 2009. (B) Scheme for the SeO_3^{2-} reduction process, TEM images of monodisperse Ag_2Se QDs with different sizes (synthesized at a 6 : 1 (left), 5 : 1 (middle), and 4 : 1 (right) molar ratio of the Ag precursor to Se precursor), and fluorescence images of a nude mouse with Ag_2Se QDs injected into the abdominal cavity. Reproduced from ref. 100 with permission from American Chemical Society, copyright 2012. (C) The glutathione metabolic pathway in yeast cells and fluorescence microscopy images of WT (above) and P_{GAL1}-*GSH1* (below) yeast cells after biosynthesis of CdSe QDs (scale bars: 10 μm). Reproduced from ref. 19 with permission from American Chemical Society, copyright 2013. (D) Mechanism of CdSe QD biosynthesis in yeast cells overexpressing MET6, and fluorescence microscopy images of WT (left) and P_{GAL1}-*MET6* cells (scale bar: 5 μm). Reproduced from ref. 95 with permission from Tsinghua University Press and Springer-Verlag GmbH Germany, part of Springer Nature, copyright 2018.

formed by the reaction of added $CdCl_2$ and GSH at the appropriate moment led to the formation of CdSe QDs in the seleniumized yeast cells. To further verify the significance of GSH, NADPH and GR in QD biosynthesis, the group realized the controlled synthesis of PbSe nanocrystals[99] and ultrasmall near-infrared Ag_2Se QDs[100] using a quasi-biosystem. Na_2SeO_3, GSH, NADPH and GR were mixed with the precursor of Pb or Ag under inert gas protection, and size-tunable PbSe or Ag_2Se QDs were obtained by adjusting the proportion of precursors. Because the fluorescence emission of the prepared Ag_2Se QDs was located in the NIR region and they had strong tissue penetration ability, the Ag_2Se QDs could be applied in *in vivo* fluorescence imaging with a high signal-to-noise ratio (Fig. 4B).

It seems that the GSH metabolic pathway plays an important role in the biosynthesis of QDs in yeast cells. Yong Li and coworkers investigated in detail the vital role of the GSH metabolic pathway in CdSe QD biosynthesis by yeast cells (Fig. 4C), and proved that engineering GSH metabolism could construct a more efficient biofactory for CdSe QD synthesis.[19] They found that during the biosynthesis of QDs, the expression of the GSH1 gene was up-regulated and the intracellular content of glutathione was also synergistically regulated. Compared with the WT strain, the glutathione metabolic mutant strains showed a significant decrease in the biosynthetic yield of CdSe QDs and their fluorescence intensity. In turn, inducing the GSH1 gene can significantly promote GSH content in the engineered cells which eventually gave a significantly higher yield of CdSe QDs. Se metabolism is another key factor for biosynthesis of CdSe QDs. Min Shao *et al.* proved that selenocysteine (SeCys) is the primary Se-precursor in the intracellular biosynthesis of CdSe QDs in yeast cells, and the synthesis yield could be improved by regulating the selenomethionine (SeMet)-to-SeCys pathway (Fig. 4D).[95] The production of biosynthesized CdSe QDs was obviously improved by the overexpression of the MET6 gene, which encoded methionine synthase and adjusted Se metabolism. Referring to CdTe QDs, through simply incubating with $CdCl_2$ and Na_2TeO_3, cells of *Saccharomyces cerevisiae* were reported to produce CdTe QDs extracellularly with high crystallinity, good water solubility, great stability, and biocompatibility.[97] In that work, the formation of QDs was observed to be more rapid at a relatively high temperature (35 °C), and the particle size and emission wavelength could be tuned *via* simply changing the incubation time.

In addition to QDs, some other nanomaterials were synthesized *via* biomineralization or direct chemical reaction on the surface of or inside yeast cells. Abundant glycoproteins and

peptidoglycans are located on the surface of yeast cells, which can locally accumulate metal ions and serve as reservoirs for the formation of metal–organic framework (MOF) crystals.[101] Kang Liang *et al.* constructed a MOF material (zeolitic imidazolate framework-8 or ZIF-8) mineralized on the surface of living yeast cells under mild conditions (Fig. 5A).[102] Later, in another study, the group fabricated a bioactive synthetic porous shell, containing a β-galactosidase (β-gal) layer and an outer MOF coating, to enable yeast cells to survive in nutrient-depleted and inhospitable environments.[103] In addition, mesoporous silica nanoparticles (MSNs) were also reversibly encapsulated onto yeast cells, through click reactions between cell-surface polysaccharides containing *cis*-diols and phenylboronic acid-linked MSNs, to protect the yeast cells in harsh environments (Fig. 5B).[104] Xiaoming Ma *et al.* constructed a living cell-based functional platform with biogenetic intracellular hydroxyapatite nanoscaffolds (nHAP@yeasts) *via* biomineralization.[105] By incubating with Na_3PO_4 under a basic environment, the yeast cells pretreated with $CaCl_2$ formed HAP nanoparticles intracellularly, maintaining good viability and proliferation ability as well as the naive yeast cells. The constructed nHAP@yeasts with good biocompatibility, hypoxia-targeting ability and high drug loading capacity were further functionalized with a targeting ligand (*i.e.*, folic acid (FA)) and loaded with a therapeutic agent (*i.e.*, DOX). The DOX-nHAP@yeasts-FA showed dual responsive profiles based on the FA dependency of tumors and the pH-sensitivity of HAP nanoparticles, and obviously inhibited tumor growth with little toxicity to normal tissues (Fig. 5C). Moreover, yeast cells have also been utilized to biosynthesize various nanomaterials such as Ag nanoparticles and Se nanoparticles.[106]

Synthesis by other fungi

In addition to yeasts, many other fungi have also demonstrated the ability to synthesize inorganic nanomaterials. CdS_xSe_{1-x} QDs with a uniform spherical shape of 3.22 ± 0.07 nm diameter were synthesized by *Phomopsis* sp. XP-8 in a Na_2SeO_3 and $CdCl_2$ aqueous solution within 6 h (Fig. 6A).[107] Several fungi including *Coriolus versicolor*,[90] *Phanerochaete chrysosporium*,[108] and *Trametes versicolor*[91] have been employed to synthesize CdS QDs, while *Aspergillus flavus*[89] and *Fusarium oxysporum* (*F. oxysporum*)[109] have been used to fabricate ZnS QDs, and also *F. oxysporum* to produce CdSe QDs.[17] When incubated with $CdCl_2$ and Na_2SeO_3 in equimolar concentrations from 0.25 to 5 mM, *F. oxysporum* produced CdSe QDs in the mycelial cells with a dose-dependent increase in fluorescence intensity, while decreased fluorescence intensity was observed at concentrations higher than 5 mM.[17] Smaller increases of reactant concentrations led to an increasing nanoparticle yield, but high amounts of metal ions might suppress the metabolism of *F. oxysporum* and inhibit biosynthesis. Besides, when cultured in solutions with pH varying from 4.0 to 9.0, the mycelial cells of *F. oxysporum* synthesized CdSe QDs with the highest fluorescence intensity at pH 7.5. Moreover, CdSe QDs with a higher fluorescence intensity were also obtained when *F. oxysporum* was incubated at 25 °C, rather than 30 or 37 °C (Fig. 6B). The researchers proposed that higher temperature induced faster precipitation speed of CdSe in the solution, thus forming smaller particles which showed lower fluorescence intensity, or the higher temperature may have influenced the metabolism of *F. oxysporum* and inhibited biosynthesis. Although biosynthesis of QDs has been demonstrated extensively in both bacteria and fungi, it seems that fungi prefer to synthesize nanomaterials

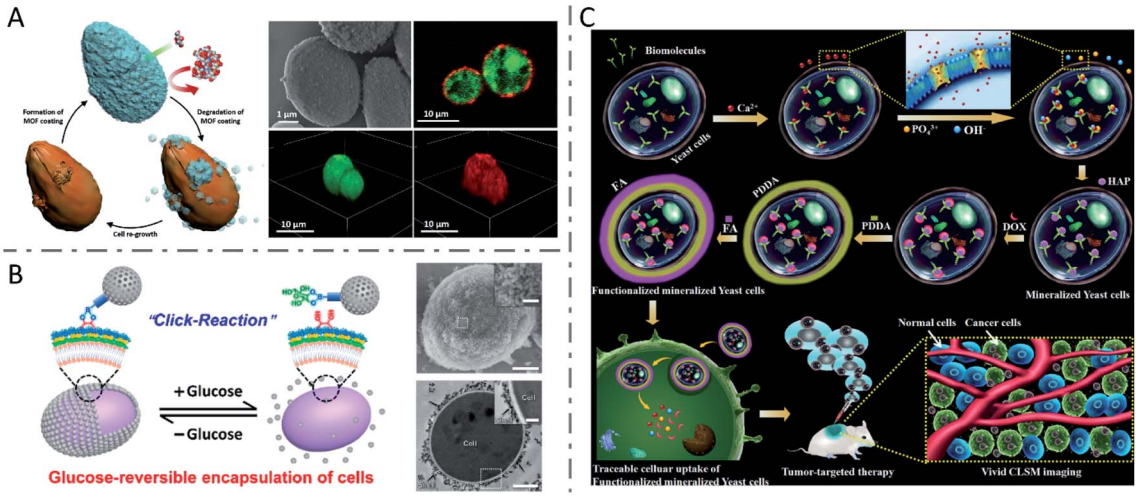

Fig. 5 Inorganic nanomaterials synthesized *via* biomineralization or direct chemical reaction in yeast cells. (A) Biomimetic crystallization of cytoprotective MOF coatings on living cells, and the SEM image and CLSM images of ZIF-8 coated yeast cells. The living yeast cells were labeled with FDA (green) and the ZIF-8 coatings were labeled by infiltration of Alexa Fluor 647 fluorescent dye (red). Reproduced from ref. 102 with permission from WILEY-VCH Verlag GmbH & Co. KGaA, Weinheim, copyright 2016. (B) Reversible encapsulation of yeast cells with MSNs using a boronic acid vicinal-diol-based click reaction, and the SEM image (scale bars: 1 μm and 200 nm (inset)) and TEM image (scale bars: 1 μm and 300 nm (inset)) of an encapsulated yeast cell. Reproduced from ref. 104 with permission from American Chemical Society, copyright 2019. (C) Formation mechanism of nHAP mineralized yeast cells and functionalized mineralized yeast cells, and their potential application in tumor-targeting delivery. Reproduced from ref. 105 with permission from The Royal Society of Chemistry, copyright 2018.

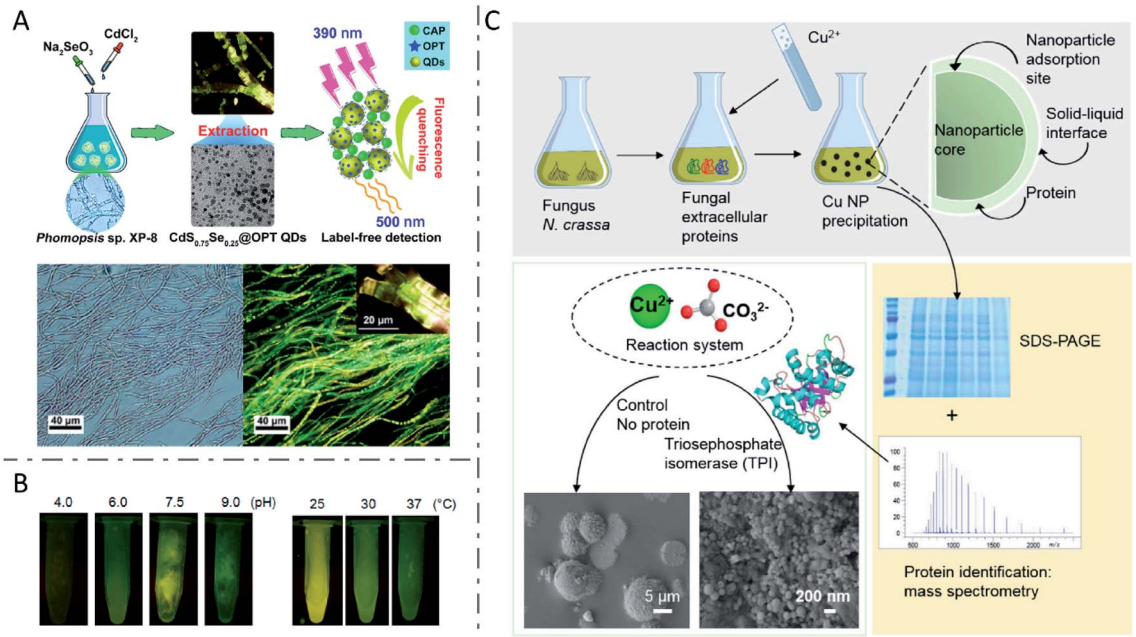

Fig. 6 Inorganic nanomaterials synthesized by fungi. (A) Biosynthesis of fluorescent CdS_xSe_{1-x} QDs by *Phomopsis* sp. XP-8 and application in label-free detection. Reproduced from ref. 107 with permission from American Chemical Society, copyright 2020. (B) CdSe QDs with tunable fluorescence intensity by changing pH and temperature. Reproduced from ref. 17 with permission from MDPI, copyright 2016. (C) The function of fungal protein TPI in controlling the morphology and structure of biosynthesized $CuCO_3$ nanoparticles *via* biomineralization. Reproduced from ref. 111 with permission from Elsevier Inc., copyright 2020.

extracellularly, due to their high amounts of bioactive secretion proteins.[108–110]

Recently, Feixue Liu *et al.* revealed the vital function of the fungal protein triosephosphate isomerase (TPI) in controlling the morphology and structure of biosynthesized $CuCO_3$ nanoparticles *via* a biomineralization process (Fig. 6C).[111] Fungus *F. oxysporum* was investigated extensively for the biosynthesis of nanomaterials such as crystalline magnetite particles,[112] ZrO_2 nanoparticles,[113] SiO_2 nanoparticles,[114] TiO_2 nanoparticles,[114] and Ag nanoparticles.[115,116] It was reported that the production of Ag nanoparticles by *F. oxysporum* was related to NR and a shuttle quinone extracellular process,[116] as well as the enzymatic generation of extracellular superoxides,[115] suggesting that multiple mechanisms may be involved. Besides, miscellaneous nanomaterials including Au,[117] Ag,[87,110,118,119] alloy-type Au/Ag nanoparticles,[88] TiO_2 nanoparticles,[120] and Te and Se nanoparticles[121] have been manufactured by fungi such as *Penicillium brevicompactum* (*P. brevicompactum*),[117] *Cladosporium cladosporioides*,[110] *Catharanthus roseus*,[118] *Phenerochaete chrysosporium*,[119] *Neurospora crassa*,[88] *Aspergillus flavus*,[120] *Aureobasidium pullulans*, *Mortierella humilis*, *Trichoderma harzianum* and *Phoma glomerata*.[121]

Since most fungi are multicellular organisms with relatively complex structures, yeasts with a simple unicellular structure are more similar to bacteria with the advantages of facile cultivation and easy genetic manipulation. It's also easier to isolate and characterize the synthesized NMs by unicellular organisms. Both bacteria and fungi can biosynthesize a variety of metallic and metalloid nanomaterials as well as their oxides and chalcogenides with a reported similar mechanism. However, in terms of scale up, fungi seem to be better candidates, because they can tolerate higher metal concentrations than bacteria and secrete a large amount of extracellular proteins and enzymes, resulting in higher production of inorganic nanomaterials.[122] Furthermore, the untapped biodiversity of fungi endows them with potential to provide different kinds of nanomaterials. In the field of tumor-targeting therapy, the capping agents of the synthesized nanomaterials originating from fungi are less likely to induce an immune response like that induced by bacteria as mentioned above.[92]

Synthesis by animal cells

The animal cell is another kind of biofactory for inorganic nanomaterial manufacturing. Compared to bacteria and fungi, nanomaterials synthesized by animal cells are scarcely investigated, due to their relatively low proliferation rate, laborious and time-consuming culture procedures, and higher cultivation cost. However, since balancing the efficacy and safety of microbial products remains a big challenge, nanomaterials synthesized by animal cells are much safer due to the same species of origin as treated subjects. Besides, the biosynthesized nanomaterials always showed unique characteristics related to the original cells, which is beneficial for tumor-targeting theranostics.

Synthesis by cancer cells

In 2005, Anshup *et al.* reported the intracellular synthesis of nanoparticles using mammalian cells for the first time.[123] They

synthesized Au nanoparticles of 20–100 nm diameter using human embryonic kidney cell HEK-293 and human cancer cells (*i.e.* HeLa, SiHa and SKNSH cells) with their cell membranes remaining intact. Subsequently, several cancer cell lines, such as HeLa,[124] HepG2,[125] MCF-7,[126] B16F10,[127] A549,[15] HCT-116 (ref. 15) and U87 (ref. 128), were used to study the biosynthesis of various nanomaterials. By incubating with $AgNO_3$ and Na_2S for only 20 minutes separately in sequence, followed by an aging process, HepG2 cells successfully synthesized Ag_2S QDs intracellularly.[125] It was noted that the intracellular synthetic yield grew with the prolongation of aging time, reached the maximum at 16 h, and then levelled off. Results also showed that the formation of QDs was accompanied by the consumption of intracellular GSH. Through a so-called spatiotemporal coupling strategy, Ling-Hong Xiong *et al.* employed living MCF-7 cancer cells to synthesize fluorescent CdSe QDs intracellularly.[126] They proposed a similar mechanism to bacterial and fungal biosynthesis involving selenite reduction metabolism and Cd^{2+} detoxification. Following a budding process, illuminated cell-derived microvesicles were obtained with QDs inside. Extracellular vesicles derived from mammalian cells have excellent stability, biocompatibility, lower immunogenicity and unique bioinformation from their parent cells, and have been widely employed for tumor-targeting drug delivery and antitumor immunotherapy.[129–134] In a recent study, AuNPs were intracellularly synthesized in melanoma B16F10 cells, and further shed to the extracellular environment with tumor antigens retained (AuNP@B16F10).[127] The AuNP-trapped vesicles were further introduced into dendritic cells (DCs), thus generating DC-derived Au nanoparticles ($AuNP@DC_{B16F10}$) with improved immunological properties, enhanced biocompatibility and stealth. With NIR laser irradiation, the constructed $AuNP@DC_{B16F10}$ could realize an efficient combination of AuNP-mediated PTT and tumor antigen-based immunotherapy, with a significant effect on the elimination of primary tumors, as well as the inhibition of tumor recurrence and metastasis (Fig. 7).

In addition, a variety of nanoclusters synthesized by animal cells have also been reported. Donghua Chen *et al.* demonstrated that cancerous cells rather than noncancerous cells spontaneously synthesized luminescent Pt NCs upon incubation with H_2PtCl_6 solution.[15] Specific fluorescence of Pt NCs synthesized in xenografted tumors after subcutaneous injection or intravenous injection of H_2PtCl_6 solutions was also observed. When combined with porphyrin derivatives as photothermal agents, the *in situ* synthesized Pt NCs realized effective fluorescence imaging and guided photothermal therapy of tumors. Later, with the addition of $Eu(NO_3)_3$ solution, a fluorescent Eu complex was also found to be spontaneously biosynthesized in both cancerous cells and tumors.[135] After entering the cells through calcium ion channels, Eu(III) ions were reduced to a low-valence state under the relatively high level of oxidative stress and the increased level of GSH in the special microenvironment of tumor cells (Fig. 8A). GR and NADPH might also be involved as reducing equivalents. Moreover, metallic nanomaterials such as Au NCs,[11,128,136] Ag NCs[124] and Cu NCs[137] have also been synthesized by cancer cells and applied for tumor-targeting imaging or/and therapy. In another study, cultured cancerous cells such as HeLa, U87 and HepG2, as well as the tumors of xenografted nude mice could synthesize fluorescent ZnO NCs and superparamagnetic Fe_3O_4 NCs when incubated or injected with zinc gluconate and $FeCl_2$ solution, while the noncancerous cell L02 or normal tissues could not, which can be explained by the specific redox homeostasis of cancer cells.[138] The relatively high concentrations of reactive oxygen species (ROS) such as H_2O_2 in cancer cells might cause the partial oxidation of Fe^{2+} and lead to the formation of Zn and Fe oxides, which could induce the specific fluorescence signal, enhanced MRI contrast and X-ray computed tomography (CT) contrast in tumors of xenografted tumor mice (Fig. 8B). It was

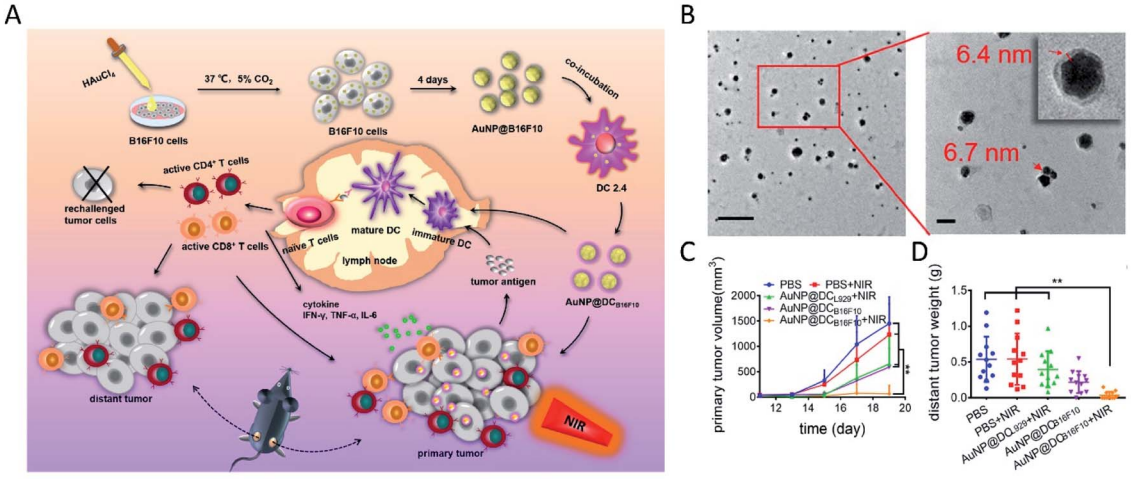

Fig. 7 Immunological Au nanoparticles synthesized by animal cells for combinatorial photothermal therapy and immunotherapy against tumors. (A) Schematic preparation of $AuNP@DC_{B16F10}$ and the mechanism of $AuNP@DC_{B16F10}$-mediated combinational treatment modality. (B) TEM images of $AuNP@DC_{B16F10}$ (scale bars: 200 and 50 nm, respectively). (C) Growth curves of the primary tumor. (D) Weight of the distant tumor harvested on 19th day. Reproduced from ref. 127 with permission from American Chemical Society, copyright 2019.

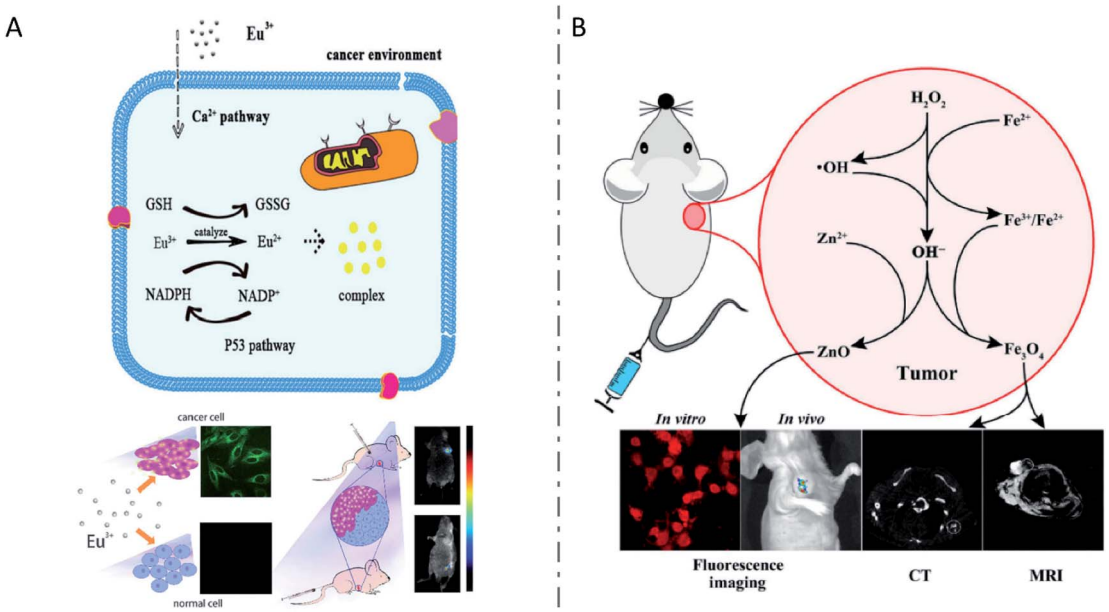

Fig. 8 Inorganic nanomaterials synthesized by animal cells. (A) The biological pathways of the biosynthesized fluorescent Eu complex by cancer cells and application in tumor bioimaging. Reproduced from ref. 135 with permission from The Royal Society of Chemistry, copyright 2016. (B) *In situ* biosynthesis of Zn & Fe oxide nanoclusters and subsequent *in vivo* multimodal bioimaging of cancer cells. Reproduced from ref. 138 with permission from Tsinghua University Press and Springer-Verlag Berlin Heidelberg, copyright 2017.

demonstrated that *in situ* biosynthesis of iridium and iron oxide nanoclusters in cancer cells or tumor tissue could be realized in a similar way for tumor-targeting multimodal bioimaging.[139] In particular, they found exosomes with internalized IrO_2 and Fe_3O_4 NCs from the serum of xenograft mice after injection, which could be used as cancer biomarkers. In addition, the *in situ* synthesis of inorganic nanomaterials such as fluorescent ZnO NCs[140,141] and magnetic Fe_3O_4 NCs[141] was also reported in lesion areas of Alzheimer's mice, for the rapid and early diagnosis of Alzheimer's disease.

Synthesis by normal cells

Besides cancer cells, some normal cells such as human mesenchymal stem cells (MSCs)[142] and platelets[143] are also reported to be utilized for biosynthesis of inorganic nanomaterials with the assistance of engineering technology or external energy stimulation. After being transfected with the *mms6* gene derived from *Magnetospirillum magneticum* AMB-1, the MSCs were found to successfully synthesize magnetic nanoparticles intracellularly, without any deleterious effects.[142] In a study on platelets, Au nanoparticles were synthesized in living platelets exposed to $HAuCl_4$, with the assistance of ultrasound energy and addition of reducing agents ($NaBH_4$ and sodium citrate).[143]

Considering the toxicity of bacterial and fungal products, nanomaterials synthesized by animal cells could be safer and more efficient for *in vivo* tumor-targeting applications due to the homology and homing effects. However, the large-scale preparation of nanomaterials synthesized by animal cells still faces great challenges, such as the high-cost, time-consuming and laborious cell cultivation and the low synthesis efficiency.[144]

Synthesis by plant cells

Many living plants can absorb metal ions and then convert them to their insoluble form to mitigate environmental stress, thus resulting in biosynthesized NMs.

Synthesis by higher plants

In most cases, the metal ions were reduced to metallic nanomaterials within living plants. Therefore, researchers gave intensive attention to nanoparticle biosynthesis by living plant cells, among which Au nanoparticles[16,145] and Ag nanoparticles[146] were the majority. In 2002, alfalfa plants were reported to produce crystalline Au nanoparticles when grown on a gold-enriched agar system, which was the first demonstration of Au nanoparticles synthesized by living plants.[147] Then, the same group reported the first biosynthesis of Ag nanoparticles by living alfalfa plants in 2003.[148] Sharma *et al.* observed the intracellular formation and growth of spherical Au nanoparticles with diameters of 6–20 nm in *Sesbania drummondii* (*S. drummondii*) exposed to $KAuCl_4$ solution (Fig. 9A), which could be explained by the reduction and stabilization by alkaloids or other secondary metabolites.[149] In a study on Au nanoparticles synthesized by diverse plant species, it was found that changes in pH of culture media had little influence on the average sizes of the synthesized Au nanoparticles, but increases in the amounts of triangular and hexagonal nanoparticles were observed at low (3.8) and high (7.8) pH, respectively.[16] Besides, lower temperature induced larger particle size and higher percent of gold nanorectangle formation with the temperature varying from 15 to 37 °C, which might be related to the effects of temperature on the growth responses and nutrient uptake by plants.

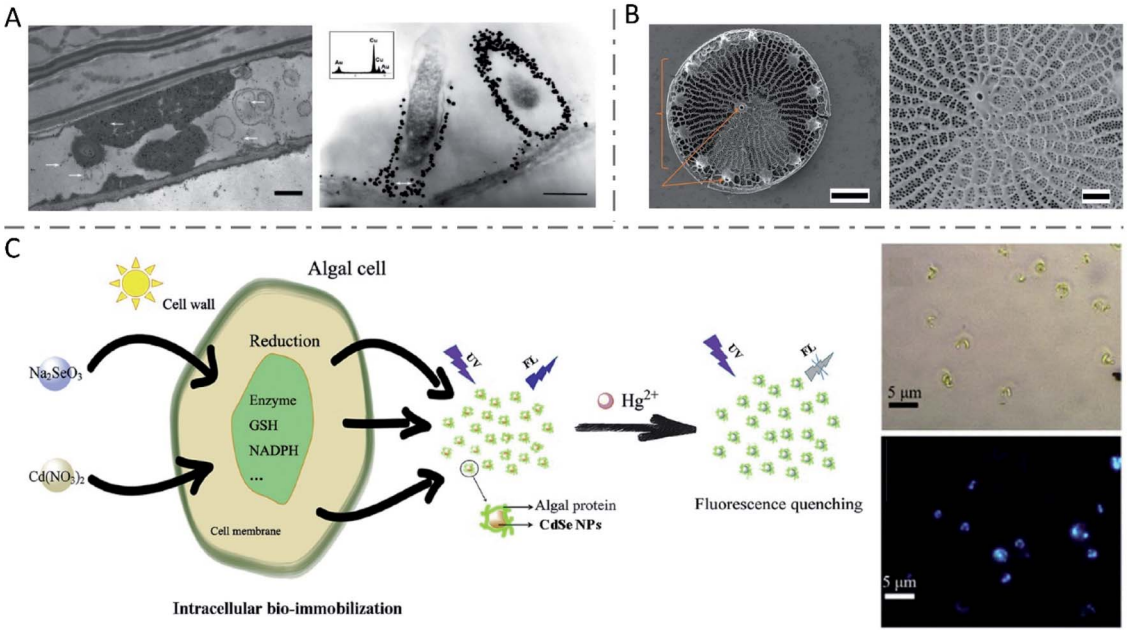

Fig. 9 Inorganic nanomaterials synthesized by plant cells. (A) TEM images of *S. drummondii* root cells loaded with gold nanoparticles (scale bars: 1 μm and 500 nm). The inset shows the EDS spectrum with gold and copper peaks (copper peaks arise from the copper grid that holds the plant tissue). Reproduced from ref. 149 with permission from American Chemical Society, copyright 2007. (B) SEM images of wild-type *Thalassiosira pseudonana* diatom (scale bars: 1 μm and 300 nm, respectively). Reproduced from ref. 155 with permission from Springer Nature, copyright 2019. (C) The synthesis of CdSe NPs by algal cells and application in Hg^{2+} detection. Reproduced from ref. 166 with permission from Elsevier B.V., copyright 2019.

The reduction of metal ions by the reductive components of living plants is the commonly accepted molecular mechanism for the formation of nanomaterials. Therefore, the contents of some reducing sugars and antioxidant compounds also played key roles in the construction of synthesized nanomaterials. Isabel R. Beattie and Richard G. Haverkamp demonstrated the synthesis of Au and Ag nanoparticles in all the tissues of *Brassica juncea* (*B. juncea*), including leaves, stems, and roots, after growing in $AuNO_3$ or $HAuCl_4$ solution.[20] They found that the nanoparticles preferred to grow in or around chloroplasts, the production center and a repository of reducing sugars (glucose and fructose) produced by photosynthesis. The quantity of these sugars in the plant seemed to influence the metal reduction processes and found to be responsible for the amount of metallic nanoparticles formed in total. However, another research study revealed that the contents of reducing sugars and antioxidant compounds, proposed to be involved in the biosynthesis of metallic nanoparticles, were quite different among three species of plants which could synthesize Ag nanoparticles, leading to the concept that there is no substance that is solely responsible for the process.[146] It is thought that there are synergistic effects among different substances, such as polysaccharides, proteins, flavonoids and terpenoids. In addition, the formations of Cu nanoparticles[150] and Au–Ag–Cu alloy[151] in living plants were also studied in a few articles. Given the complexity of plant metabolism, the synthesis of nanomaterials in whole living plants is usually uncontrollable. More reports have focused on biosynthesis using plant extracts.[152–154]

Synthesis by algae cells

Algae, simple plants with no real leaves, stems or roots, have been investigated for nanoparticle biosynthesis as well.[7] Algae are easy to harvest and to culture, they grow fast, and few produce toxins like bacteria and fungi.[8] As is well known, diatoms have an innate ability to synthesize nanoscale SiO_2 to construct cell walls (Fig. 9B).[155–157] Similar to higher plants, various algae such as *Chlamydomonas reinhardtii* (*C. reinhardtii*),[158,159] *Cystophora moniliformis*,[160] and *Botryococcus braunii* (*B. braunii*)[12] have been used to biosynthesize Ag nanoparticles, while algae such as *Klebsormidium flaccidum*,[161] *Nostoc ellipsosporum*,[162] *Rhizoclonium fontinale*,[163] and *Euglena gracilis*[164] have been used to synthesize Au nanomaterials. What's different, algal resources including cell-free extracts, broths, isolated proteins and whole living cells can be used in the biosynthesis of metallic-, chalcogenide- and oxide-based nanomaterials.[8] Living cells of *C. reinhardtii* were employed to produce composition-controllable Ag–Au alloy nanoparticles with a uniform spherical shape.[165] Composition-tunable bimetallic alloys could be synthesized by simply changing the stoichiometric ratio of metal salts added to the cultures. The researchers described the extracellular alloy nanoparticle creation processes as three stages: cellular uptake of metal ions and reduction-mediated formation of nanoparticles, stabilization of the nanoparticles by the extracellular matrix around, and release of the nanoparticles to the culture medium. Similar to other species, fluorescent CdSe QDs could be efficiently synthesized by algae cells, by incubating algae cells with immobilized Cd ions with different types of selenium sources.[166,167] The possible mechanisms included the internalization of Na_2SeO_3 by an

Table 1 Summary of typical inorganic nanomaterials synthesized by various living cells

Species	Cells	Inorganic NMs	Applications	Reference
Bacteria	*Magnetospirillum magneticum* AMB-1	Fe_3O_4 NPs	T2-weighted MRI and PTT of tumors	34
	Magnetospirillum gryphiswaldense MSR-1	Fe_3O_4 NPs	MHT on carcinoma cells	38
	Escherichia coli MG1655	Au NPs	Photothermally controlled TNF-α therapy	14
	Bacillus subtilis	Ag NPs	Antibacterial activity	184
	Shewanella oneidensis MR-1	Pd NPs	Augmenting photothermal tumor therapy	64
	Lactobacillus casei ATCC 393	Se NPs	Antioxidant activity	62
	Staphylococcus aureus	Te NRs	—	41
	Escherichia coli	CdS_xSe_{1-x} QDs	Bioimaging of cancer cells and tumor tissue of mice	26
	Staphylococcus aureus	$CdS_{0.5}Se_{0.5}$ QDs	Pathogen detection	24
	Escherichia coli	CdTe QDs	—	18
	Escherichia coli	MnO_x nanospindles	MRI and enhanced cancer-specific chemo-chemodynamic therapy	46
Yeasts	*Candida glabrata* and *Schizosaccharomyces pombe*	CdS crystallites	—	94
	Saccharomyces cerevisiae BY4742	CdSe QDs	—	96
	Saccharomyces cerevisiae	CdTe QDs	—	97
	Saccharomyces cerevisiae	ZIF-8	Cytoprotective exoskeletons for living cells	102
	Saccharomyces cerevisiae	Mesoporous silica NPs	Effective living cell protection under harsh conditions	104
	—	Hydroxyapatite nanoscaffolds	Cell-based drug carrier system for tumor-targeting therapy	105
	Pichia pastoris	Ag and Se NPs	—	106
Multicellular fungi	*Phomopsis* sp. XP-8	CdS_xSe_{1-x} QDs	Chloramphenicol detection	107
	Phanerochaete chrysosporium BKMF-1767	CdS QDs	—	108
	Fusarium oxysporum	ZnS QDs	—	109
	Neurospora crassa	$CuCO_3$ NPs	—	111
	Fusarium oxysporum	ZrO_2 NPs	—	113
	Fusarium oxysporum	SiO_2 and TiO_2 NPs	—	114
	Penicillium brevicompactum	Au NPs	Cytotoxic effects against cancer cells	117
	Catharanthus roseus	Ag NPs	Anticancer properties against cancer cells	118
	Neurospora crassa	Alloy-type Au/Ag NPs	—	88
	Aureobasidium pullulans, *Mortierella humilis*, *Trichoderma harzianum* and *Phoma glomerata*	Se and Te NPs	—	121
Animal cells	Human hepatoma carcinoma cell HepG2	Ag_2S QDs	NIR fluorescence imaging	125
	Mammalian cancer cell MCF-7	CdSe QDs	Fluorogenic labeling	126
	Melanoma cell B16F10	Au NPs	Combinatorial photothermal therapy and immunotherapy against tumors	127
	Platelets	Au NPs	Dark-field microscopy (DFM)-based imaging and CT imaging	143
	Human hepatocarcinoma cell HepG2 and lung cancer cell A549	Pt NCs	Fluorescence imaging and photothermal therapy of tumors	15
	Human hepatocarcinoma cell HepG2	Eu complex	Fluorescence imaging of tumors	135
	Human breast carcinoma cell MDA-MB-231	Cu NCs	Intracellular temperature nanoprobes	137
	HeLa, U87, and HepG2 cancer cells	ZnO and Fe_3O_4 NCs	Fluorescence imaging, CT imaging and MRI of tumors	138
	HeLa and HepG2 cancer cells	IrO_2 and Fe_3O_4 NCs	Fluorescence imaging, CT imaging and MRI of tumors	139
	Human mesenchymal stem cells	Fe_3O_4 NPs	MRI	142
Higher plants	*Sesbania drummondii*	Au NPs	Catalytic function	149
	Brassica juncea	Au and Ag NPs	—	20
	Phragmites australis and *Iris pseudoacorus*	Cu NPs	—	150
	Brassica juncea	Au–Ag–Cu alloy	—	151
Algae	Diatom *Thalassiosira pseudonana*	SiO_2	—	157
	Klebsormidium flaccidum	Au NPs	—	161
	Cystophora moniliformis	Ag NPs	—	160
	Chlamydomonas reinhardtii	Ag–Au alloy NPs	—	165
	Chlorella pyrenoidosa and *Scenedesmus obliquus*	CdSe QDs	Fluorescent nanoprobe for imatinib detection	167
	Chlorella kessleri	Cu and CuO NPs	—	168
	Chlorella sp. HQ	Fe-based NMs	Harvesting of oleaginous microalgae	170

Table 2 Summary of factors affecting the synthesis of inorganic nanomaterials by living cells

Cells	Inorganic NMs	Regulated characteristics	Affecting factors	Reference
Escherichia coli DH5α	FeCo metal NPs	Size	Concentration of Fe^{2+} (or Fe^{4+}) and Co^{2+} metal ions	21
Escherichia coli DH5α	CdSe NPs	Size, color and fluorescence emission wavelength	Concentration of Cd^{2+} and Se^{+} metal ions	21
Escherichia coli DH5α	ZnO, $BaCO_3$, Eu, Gd NMs, *etc.*	Producibility and crystallinity	Reduction potential and pH	40
Escherichia coli K12	CdTe QDs	Size and fluorescence emission wavelength	Incubation time	18
Escherichia coli	CdS_xSe_{1-x} QDs and $Cd_3(PO_4)_2$	Synthesis rate and yield	Glucose metabolism	26
Shewanella oneidensis MR-1	CdSe QDs and Se NPs	Synthetic yield	Engineering to regulate extracellular electron transfer ability	23
Saccharomyces cerevisiae	CdSe QDs	Size and fluorescence wavelength	Incubation time	96
Saccharomyces cerevisiae	CdTe QDs	Size and fluorescence wavelength; synthesis rate	Incubation time; temperature	97
Saccharomyces cerevisiae	CdSe QDs	Synthesis yield	Engineering to regulate Se metabolism	95
Saccharomyces cerevisiae	CdSe QDs	Synthesis yield	Engineering to regulate glutathione metabolism	19
Fusarium oxysporum	CdSe QDs	Fluorescence intensity, size, synthesis rate and yield	Concentration of $CdCl_2$ and Na_2SeO_3, pH, and temperature	17
Human hepatoma carcinoma cell HepG2	Ag_2S QDs	Synthetic yield and fluorescence intensity	Aging time	125
Medicago sativa (alfalfa)	Au NPs	Shape and size	pH, temperature and light conditions	16
Botryococcus braunii	Ag NPs	Crystallinity, shape, size, yield and synthetic rate	Concentration of $AgNO_3$ and pH	12

osmotic process, the generation of selenium precursors by the reduction reaction in the thylakoid membranes or cytoplasm within the electron transport system (ETS), the combination of selenium precursors and $Cd(SG)_2$ under the catalysis of relative reductase to form CdSe nanoparticles with protective protein molecules, and the accumulation in the algal cytoplasm or release into culture media.[166] Since the obtained QDs showed obvious fluorescence quenching by Hg^{2+}, they were successfully employed for Hg^{2+} detection (Fig. 9C). In addition, some articles also demonstrated the biofabrication of Cu and CuO nanoparticles,[168] superparamagnetic 2-line ferrihydrite nanoparticles[169] and Fe-based magnetic nanomaterials[170] by algae cells.

The synthesis of nanomaterials in whole living plants is usually uncontrollable and inhomogeneous, and thus difficult in practical application. Algae, which are generally unicellular, colonial or constructed of filaments or composed of simple tissues, have the advantages of being easy to harvest and to culture, and produce no toxins, making it possible for scalable, sustainable and eco-friendly bioproduction of safer nanomaterials.[8]

Viral synthesis

Viruses are nanosized non-cellular organisms, typically consisting of self-assembled capsid proteins (CPs) surrounding an RNA or DNA core of genetic material.[171] Since viruses have no cellular structure, the biosynthesis of nanoparticles in them is distinct from that in living cells discussed above, and cannot be veritably called "living cell synthesis". In general, viruses serve as templates or scaffolds for metal nanoparticle biomineralization, because of their extremely tiny sizes and bioactive protein surfaces.[172] Besides, genetic modification[173] and chemical modification[174] can be used to functionalize the obtained virus-based nanomaterials. M13 filamentous bacteriophages have been widely used to synthesize a variety of inorganic nanoparticles, such as Au nanostructures,[175–177] Ag nanoparticles,[173] Cu nanostructures[178] and Co–Pt alloy nanoparticles.[179] Furthermore, tobacco mosaic viruses,[180,181] potato virus X[182] and cowpea chlorotic mottle viruses[183] have also been utilized in templated synthesis of nanomaterials.

Conclusions

In this review, we summarized the biosynthesis of inorganic nanomaterials in different types of living cells including bacteria, fungi, plant cells and animal cells, accompanied by their application in tumor-targeting theranostics (Table 1). The mechanisms involving inorganic-ion bioreduction and detoxification as well as biomineralization are emphasized. Based on the mechanisms, we describe the size and morphology control of the products *via* the modulation of precursor ion concentration, pH, temperature, and incubation time, as well as cell

metabolism by a genetic engineering strategy (Table 2). Compared to the conventional chemical synthesis, living cell synthesis has the advantages of easy preparation and environmental friendliness. Meanwhile, the obtained biosynthetic nanomaterials have the characteristics of good biocompatibility and unique biological properties. When it comes to bacteria, characteristics of single cell growth, facile cultivation, rapid proliferation, and particularly easy genetic manipulation make it possible to synthesize designed nanomaterials under mild conditions. The inherent tumor-targeting ability and immune response activation of bacteria also contribute to the targeted diagnosis and treatment of tumors by bacteria-synthesized nanomaterials. Compared with other microorganisms, fungi are more tolerant to metal ions, and secrete more extracellular enzymes and proteins, resulting in higher yields of nanomaterials and easier scale-up production. Considering the toxicity of bacterial and fungal products, nanomaterials synthesized by animal cells could be safer and efficient for *in vivo* tumor-targeting applications due to the homology and homing effects. Referring to synthesis by plant cells, few produce toxins like bacteria and fungi, leading to scalable, sustainable and eco-friendly bioproduction of nanomaterials. Despite the emerged limitations, such as the controllability of the biosynthetic process and safety of biological components, inorganic nanomaterials synthesized by living cells show a great promise for biomedical applications.

Perspectives

In spite of what is mentioned above, it is still a far way to go until inorganic nanomaterials synthesized by living cells predominate the field of tumor-targeting applications. Researchers should pay more attention to the following aspects. (1) The mechanisms of inorganic nanomaterial synthesis in living cells are reported to be mainly related to inorganic-ion bioreduction, detoxification and biomineralization. Some kinds of intracellular enzymes, reducing molecules such as glutathione and glucose, cell surface expressed polysaccharides and proteins are proved to participate in these biosynthetic processes and play key roles. However, the biochemical reactions involved are so complicated that the mechanisms are not illustrated deeply in most cases. For the purpose of controllable preparation, the mechanisms should be clearly clarified. (2) Referring to the controllability of biosynthesis, it is a more challenging issue. As we all know, the components, size, morphology, purity *etc.* have crucial impacts on the properties of nanomaterials. Likewise, their surface coating and stability are also important for their bioapplication. How can we make the living cells give us what we want but not what they can? Modulation of precursor ion concentration, pH, temperature, and incubation time, as well as cell metabolism by genetic engineering can help to some extent, but more strategies are urgently needed. (3) Majority of the biosynthetic products are metallic nanoparticles and their oxides or chalcogenides. However, functional inorganic nanomaterials that can be used in biomedicine and other fields are far more diverse than these. Considering the diversity of living cells, the bioconstruction of many other types of nanomaterials would become possible. (4) Although there are many advantages of biosynthesis, high-quality inorganic nanomaterials are usually prepared by chemical processes. Under mild reaction conditions, the crystal orientation of the available nanomaterials will not be as perfect as those fabricated at high temperature. The presence of defects will degrade the performance of the nanomaterials. (5) Biosynthesis is considered as a cost-effective and eco-friendly approach for inorganic nanomaterial preparation. It is highly possible to scale up the synthesis. But before that, the process parameters should be optimized and the preparation technology needs to be deeply investigated. (6) The capping agents on the surface of nanomaterials originating from living cells during the biosynthesis endow them with high stability and good biocompatibility. Sometimes, they can synergize with the nanomaterials to enhance their therapeutic effect, for example, the immune response activation by lipopolysaccharides on the outer membrane of bacteria. On the other hand, as exogenous biomolecules, their potential toxicity should be considered. (7) When it comes to their commercial application, standards regarding biofabrication, characterization, evaluation and so on of the nanomaterials should be established.

Conflicts of interest

There are no conflicts to declare.

Acknowledgements

This work was financially supported by National Natural Science Foundation of China (81771978, 82072066 and 81627901), National Key Research and Development Program of China (2018YFA0208903 and 2020YFA0710700).

Notes and references

1 Y. Zhang, W. Zhang, K. Zeng, Y. Ao, M. Wang, Z. Yu, F. Qi, W. Yu, H. Mao, L. Tao, C. Zhang, T. T. Y. Tan, X. Yang, K. Pu and S. Gao, *Small*, 2020, **16**, e1906797.
2 Y. Zhang, C. Xu, X. Yang and K. Pu, *Adv. Mater.*, 2020, **32**, e2002661.
3 X. Zhong, X. Wang, G. Zhan, Y. Tang, Y. Yao, Z. Dong, L. Hou, H. Zhao, S. Zeng, J. Hu, L. Cheng and X. Yang, *Nano Lett.*, 2019, **19**, 8234–8244.
4 H. Zhao, J. Xu, W. Huang, G. Zhan, Y. Zhao, H. Chen and X. Yang, *ACS Nano*, 2019, **13**, 6647–6661.
5 Y. Tang, T. Yang, Q. Wang, X. Lv, X. Song, H. Ke, Z. Guo, X. Huang, J. Hu, Z. Li, P. Yang, X. Yang and H. Chen, *Biomaterials*, 2018, **154**, 248–260.
6 A. S. Mathuriya, *Crit. Rev. Biotechnol.*, 2016, **36**, 788–802.
7 K. Vijayaraghavan and T. Ashokkumar, *J. Environ. Chem. Eng.*, 2017, **5**, 4866–4883.
8 S. A. Dahoumane, M. Mechouet, K. Wijesekera, C. D. M. Filipe, C. Sicard, D. A. Bazylinski and C. Jeffryes, *Green Chem.*, 2017, **19**, 552–587.
9 K. Wang, X. Zhang, I. M. Kislyakov, N. Dong, S. Zhang, G. Wang, J. Fan, X. Zou, J. Du, Y. Leng, Q. Zhao, K. Wu,

J. Chen, S. M. Baesman, K. S. Liao, S. Maharjan, H. Zhang, L. Zhang, S. A. Curran, R. S. Oremland, W. J. Blau and J. Wang, *Nat. Commun.*, 2019, **10**, 3985.
10 Q.-Y. Luo, Y. Lin, Y. Li, L.-H. Xiong, R. Cui, Z.-X. Xie and D.-W. Pang, *Small*, 2014, **10**, 699–704.
11 M. Wang, Z. Yu, H. Feng, J. Wang, L. Wang, Y. Zhang, L. Yin, Y. Du, H. Jiang, X. Wang and J. Zhou, *J. Mater. Chem. B*, 2019, **7**, 5336–5344.
12 A. Arévalo-Gallegos, J. Saul Garcia-Perez, D. Carrillo-Nieves, R. A. Ramirez-Mendoza, H. M. N. Iqbal and R. Parra-Saldivar, *Int. J. Nanomed.*, 2018, **13**, 5591–5604.
13 G. F. Luo, W. H. Chen, X. Zeng and X. Z. Zhang, *Chem. Soc. Rev.*, 2021, **50**, 945–985.
14 J.-X. Fan, Z.-H. Li, X.-H. Liu, D.-W. Zheng, Y. Chen and X.-Z. Zhang, *Nano Lett.*, 2018, **18**, 2373–2380.
15 D. Chen, C. Zhao, J. Ye, Q. Li, X. Liu, M. Su, H. Jiang, C. Amatore, M. Selke and X. Wang, *ACS Appl. Mater. Interfaces*, 2015, **7**, 18163–18169.
16 D. L. Starnes, A. Jain and S. V. Sahi, *Environ. Sci. Technol.*, 2010, **44**, 7110–7115.
17 T. Yamaguchi, Y. Tsuruda, T. Furukawa, L. Negishi, Y. Imura, S. Sakuda, E. Yoshimura and M. Suzuki, *Materials*, 2016, **9**, 855.
18 H. Bao, Z. Lu, X. Cui, Y. Qiao, J. Guo, J. M. Anderson and C. M. Li, *Acta Biomater.*, 2010, **6**, 3534–3541.
19 Y. Li, R. Cui, P. Zhang, B.-B. Chen, Z.-Q. Tian, L. Li, B. Hu, D.-W. Pang and Z.-X. Xie, *ACS Nano*, 2013, **7**, 2240–2248.
20 I. R. Beattie and R. G. Haverkamp, *Metallomics*, 2011, **3**, 628–632.
21 T. J. Park, S. Y. Lee, N. S. Heo and T. S. Seo, *Angew. Chem., Int. Ed. Engl.*, 2010, **49**, 7019–7024.
22 X. Wang, J. Pu, B. An, Y. Li, Y. Shang, Z. Ning, Y. Liu, F. Ba, J. Zhang and C. Zhong, *Adv. Mater.*, 2018, **30**, e1705968.
23 L.-J. Tian, W.-W. Li, T.-T. Zhu, J.-J. Chen, W.-K. Wang, P.-F. An, L. Zhang, J.-C. Dong, Y. Guan, D.-F. Liu, N.-Q. Zhou, G. Liu, Y.-C. Tian and H.-Q. Yu, *J. Am. Chem. Soc.*, 2017, **139**, 12149–12152.
24 J.-J. Wang, Y. Lin, Y.-Z. Jiang, Z. Zheng, H.-Y. Xie, C. Lv, Z.-L. Chen, L.-H. Xiong, Z.-L. Zhang, H. Wang and D.-W. Pang, *Anal. Chem.*, 2019, **91**, 7280–7287.
25 D. C. Vaigankar, S. K. Dubey, S. Y. Mujawar, A. D'Costa and S. K. Shyama, *Ecotoxicol. Environ. Saf.*, 2018, **165**, 516–526.
26 L.-J. Tian, Y. Min, W.-W. Li, J.-J. Chen, N.-Q. Zhou, T.-T. Zhu, D.-B. Li, J.-Y. Ma, P.-F. An, L.-R. Zheng, H. Huang, Y.-Z. Liu and H.-Q. Yu, *ACS Nano*, 2019, **13**, 5841–5851.
27 R. Blakemore, *Science*, 1975, **190**, 377–379.
28 S. Rosenfeldt, C. N. Riese, F. Mickoleit, D. Schüler and A. S. Schenk, *Appl. Environ. Microbiol.*, 2019, **85**, e01513–01519.
29 M. A. Carillo, M. Bennet and D. Faivre, *J. Phys. Chem. B*, 2013, **117**, 14642–14648.
30 D. A. Bazylinski and R. B. Frankel, *Nat. Rev. Microbiol.*, 2004, **2**, 217–230.
31 R. Uebe and D. Schüler, *Nat. Rev. Microbiol.*, 2016, **14**, 621–637.
32 M. I. Siponen, P. Legrand, M. Widdrat, S. R. Jones, W.-J. Zhang, M. C. Y. Chang, D. Faivre, P. Arnoux and D. Pignol, *Nature*, 2013, **502**, 681–684.
33 O. Felfoul, M. Mohammadi, S. Taherkhani, D. de Lanauze, Y. Z. Xu, D. Loghin, S. Essa, S. Jancik, D. Houle, M. Lafleur, L. Gaboury, M. Tabrizian, N. Kaou, M. Atkin, T. Vuong, G. Batist, N. Beauchemin, D. Radzioch and S. Martel, *Nat. Nanotechnol.*, 2016, **11**, 941–947.
34 C. Chen, S. Wang, L. Li, P. Wang, C. Chen, Z. Sun and T. Song, *Biomaterials*, 2016, **104**, 352–360.
35 E. Alphandery, D. Abi Haidar, O. Seksek, M. Thoreau, A. Trautmann, N. Bercovici, F. Gazeau, F. Guyot and I. Chebbi, *ACS Appl. Mater. Interfaces*, 2017, **9**, 36561–36572.
36 T. Tang, L. Zhang, R. Gao, Y. Dai, F. Meng and Y. Li, *Appl. Microbiol. Biotechnol.*, 2012, **94**, 495–503.
37 C. Lang and D. Schuler, *Appl. Environ. Microbiol.*, 2008, **74**, 4944–4953.
38 D. Gandia, L. Gandarias, I. Rodrigo, J. Robles-Garcia, R. Das, E. Garaio, J. A. Garcia, M. H. Phan, H. Srikanth, I. Orue, J. Alonso, A. Muela and M. L. Fdez-Gubieda, *Small*, 2019, **15**, e1902626.
39 A. Plan Sangnier, S. Preveral, A. Curcio, A. K. A. Silva, C. T. Lefèvre, D. Pignol, Y. Lalatonne and C. Wilhelm, *J. Controlled Release*, 2018, **279**, 271–281.
40 Y. Choi, T. J. Park, D. C. Lee and S. Y. Lee, *Proc. Natl. Acad. Sci. U. S. A.*, 2018, **115**, 5944–5949.
41 L.-H. Xiong, R. Cui, Z.-L. Zhang, J.-W. Tu, Y.-B. Shi and D.-W. Pang, *Small*, 2015, **11**, 5416–5422.
42 L.-J. Tian, W.-W. Li, T.-T. Zhu, G.-H. Zhao, X.-W. Liu, J.-C. Dong, P.-F. An, J.-Y. Ma, F. Shen, C. Qian, B. Hu and H.-Q. Yu, *J. Mater. Chem. A*, 2019, **7**, 18480–18487.
43 D. B. Li, Y. Y. Cheng, C. Wu, W. W. Li, N. Li, Z. C. Yang, Z. H. Tong and H. Q. Yu, *Sci. Rep.*, 2014, **4**, 3735.
44 S. Iravani and R. S. Varma, *ACS Sustainable Chem. Eng.*, 2020, **8**, 5395–5409.
45 H. J. Bai, Z. M. Zhang and J. Gong, *Biotechnol. Lett.*, 2006, **28**, 1135–1139.
46 Y. W. Bao, X. W. Hua, J. Zeng and F. G. Wu, *Research*, 2020, **2020**, 9301215.
47 L.-H. Xiong, R. Cui, Z.-L. Zhang, X. Yu, Z. Xie, Y.-B. Shi and D.-W. Pang, *ACS Nano*, 2014, **8**, 5116–5124.
48 L. Du, H. Jiang, X. Liu and E. Wang, *Electrochem. Commun.*, 2007, **9**, 1165–1170.
49 G. Attard, M. Casadesús, L. E. Macaskie and K. Deplanche, *Langmuir*, 2012, **28**, 5267–5274.
50 X. Jiang, X. Fan, W. Xu, R. Zhang and G. Wu, *ACS Biomater. Sci. Eng.*, 2020, **6**, 680–689.
51 X. Jiang, C. Zhao, X. Fan and G. Wu, *ACS Omega*, 2019, **4**, 16667–16673.
52 B. Nair and T. Pradeep, *Cryst. Growth Des.*, 2002, **2**, 293–298.
53 I. W.-S. Lin, C.-N. Lok and C.-M. Che, *Chem. Sci.*, 2014, **5**, 3144–3150.
54 R. L. Kimber, E. A. Lewis, F. Parmeggiani, K. Smith, H. Bagshaw, T. Starborg, N. Joshi, A. I. Figueroa, G. van der Laan, G. Cibin, D. Gianolio, S. J. Haigh, R. A. D. Pattrick, N. J. Turner and J. R. Lloyd, *Small*, 2018, **14**, 1703145.

55 S. Y. Chen, C. Y. Xing, D. Z. Huang, C. H. Zhou, B. Ding, Z. H. Guo, Z. C. Peng, D. Wang, X. Zhu, S. Z. Liu, Z. Cai, J. Y. Wu, J. Q. Zhao, Z. Z. Wu, Y. H. Zhang, C. Y. Wei, Q. T. Yan, H. Z. Wang, D. Y. Fan, L. P. Liu, H. Zhang and Y. H. Cao, *Sci. Adv.*, 2020, **6**, 11.

56 T. Yang, H. T. Ke, Q. L. Wang, Y. A. Tang, Y. B. Deng, H. Yang, X. L. Yang, P. Yang, D. S. Ling, C. Y. Chen, Y. L. Zhao, H. Wu and H. B. Chen, *ACS Nano*, 2017, **11**, 10012–10024.

57 W. Huang, Y. Huang, Y. You, T. Nie and T. Chen, *Adv. Funct. Mater.*, 2017, **27**, 1701388.

58 L. L. Shi, J. Y. Sheng, M. L. Wang, H. Luo, J. Zhu, B. X. Zhang, Z. Liu and X. L. Yang, *Theranostics*, 2019, **9**, 4115–4129.

59 J.-X. Fan, M.-Y. Peng, H. Wang, H.-R. Zheng, Z.-L. Liu, C.-X. Li, X.-N. Wang, X.-H. Liu, S.-X. Cheng and X.-Z. Zhang, *Adv. Mater.*, 2019, **31**, 1808278.

60 W. Chen, Y. Wang, M. Qin, X. Zhang, Z. Zhang, X. Sun and Z. Gu, *ACS Nano*, 2018, **12**, 5995–6005.

61 L. Shi, J. Sheng, G. Chen, P. Zhu, C. Shi, B. Li, C. Park, J. Wang, B. Zhang, Z. Liu and X. Yang, *J. Immunother. Cancer.*, 2020, **8**, e000973.

62 C. Xu, L. Qiao, Y. Guo, L. Ma and Y. Cheng, *Carbohydr. Polym.*, 2018, **195**, 576–585.

63 V. K. Nguyen, W. Choi, Y. Ha, Y. Gu, C. Lee, J. Park, G. Jang, C. Shin and S. Cho, *J. Ind. Eng. Chem.*, 2019, **78**, 246–256.

64 Q.-W. Chen, X.-H. Liu, J.-X. Fan, S.-Y. Peng, J.-W. Wang, X.-N. Wang, C. Zhang, C.-J. Liu and X.-Z. Zhang, *Adv. Funct. Mater.*, 2020, **30**, 1909806.

65 C.-Y. Wen, J. Hu, Z.-L. Zhang, Z.-Q. Tian, G.-P. Ou, Y.-L. Liao, Y. Li, M. Xie, Z.-Y. Sun and D.-W. Pang, *Anal. Chem.*, 2013, **85**, 1223–1230.

66 J. Hu, C.-Y. Wen, Z.-L. Zhang, M. Xie, J. Hu, M. Wu and D.-W. Pang, *Anal. Chem.*, 2013, **85**, 11929–11935.

67 X. Wu, J. Hu, B. Zhu, L. Lu, X. Huang and D. Pang, *J. Chromatogr.*, 2011, **1218**, 7341–7346.

68 J. Hu, M. Xie, C.-Y. Wen, Z.-L. Zhang, H.-Y. Xie, A.-A. Liu, Y.-Y. Chen, S.-M. Zhou and D.-W. Pang, *Biomaterials*, 2011, **32**, 1177–1184.

69 M. Xie, J. Hu, Y.-M. Long, Z.-L. Zhang, H.-Y. Xie and D.-W. Pang, *Biosens. Bioelectron.*, 2009, **24**, 1311–1317.

70 Y. Zhang, J.-Y. Xiao, Y. Zhu, L.-J. Tian, W.-K. Wang, T.-T. Zhu, W.-W. Li and H.-Q. Yu, *Anal. Chem.*, 2020, **92**, 3990–3997.

71 W. Wang, Y. Liu, T. Shi, J. Sun, F. Mo and X. Liu, *Anal. Chem.*, 2020, **92**, 1598–1604.

72 M. Wu, W. Wu, Y. Duan, X. Li, G. Qi and B. Liu, *Chem. Mater.*, 2019, **31**, 7212–7220.

73 S.-B. Wang, X.-H. Liu, B. Li, J.-X. Fan, J.-J. Ye, H. Cheng and X.-Z. Zhang, *Adv. Funct. Mater.*, 2019, **29**, 1904093.

74 D.-W. Zheng, Y. Chen, Z.-H. Li, L. Xu, C.-X. Li, B. Li, J.-X. Fan, S.-X. Cheng and X.-Z. Zhang, *Nat. Commun.*, 2018, **9**, 1680.

75 S. Yan, X. Zeng, Y. Wang and B.-F. Liu, *Adv. Healthcare Mater.*, 2020, **9**, 2000046.

76 W. Park, S. Cho, D. Kang, J. H. Han, J. H. Park, B. Lee, J. Lee and D. H. Kim, *Adv. Healthcare Mater.*, 2020, **9**, e1901812.

77 S. Suh, A. Jo, M. A. Traore, Y. Zhan, S. L. Coutermarsh-Ott, V. M. Ringel-Scaia, I. C. Allen, R. M. Davis and B. Behkam, *Adv. Sci.*, 2019, **6**, 1801309.

78 Y. Luo, D. Xu, X. Gao, J. Xiong, B. L. Jiang, Y. Zhang, Y. T. Wang, Y. Tang, C. Chen, H. Qiao, H. N. Li and J. Z. Zou, *Biochem. Biophys. Res. Commun.*, 2019, **514**, 1147–1153.

79 R. J. Li, L. Helbig, J. Fu, X. Y. Bian, J. Herrmann, M. Baumann, A. F. Stewart, R. Muller, A. Y. Li, D. Zips and Y. M. Zhang, *Res. Microbiol.*, 2019, **170**, 74–79.

80 L. Liu, H. He, Z. Luo, H. Zhou, R. Liang, H. Pan, Y. Ma and L. Cai, *Adv. Funct. Mater.*, 2020, **30**, 1910176.

81 W. F. Chen, Z. F. Guo, Y. N. Zhu, N. Qiao, Z. R. Zhang and X. Sun, *Adv. Funct. Mater.*, 2020, **30**, 1906623.

82 S. Iravani and R. S. Varma, *Green Chem.*, 2019, **21**, 4583–4603.

83 M. Sedighi, A. Z. Bialvaei, M. R. Hamblin, E. Ohadi, A. Asadi, M. Halajzadeh, V. Lohrasbi, N. Mohammadzadeh, T. Amiriani, M. Krutova, A. Amini and E. Kouhsari, *Cancer Med.*, 2019, **8**, 3167–3181.

84 P. Bonfante, F. Venice and L. Lanfranco, *Curr. Opin. Microbiol.*, 2019, **49**, 18–25.

85 H. P. Grossart, S. van den Wyngaert, M. Kagami, C. Wurzbacher, M. Cunliffe and K. Rojas-Jimenez, *Nat. Rev. Microbiol.*, 2019, **17**, 339–354.

86 M. V. Powers-Fletcher, B. A. Kendall, A. T. Griffin and K. E. Hanson, *Microbiol. Spectr.*, 2016, **4**, DMIH2-0002-2015.

87 N. Feroze, B. Arshad, M. Younas, M. I. Afridi, S. Saqib and A. Ayaz, *Microsc. Res. Tech.*, 2020, **83**, 72–80.

88 E. Castro-Longoria, A. R. Vilchis-Nestor and M. Avalos-Borja, *Colloids Surf., B*, 2011, **83**, 42–48.

89 P. Uddandarao and R. B. Mohan, *Mater. Sci. Eng., B*, 2016, **207**, 26–32.

90 R. Sanghi and P. Verma, *Chem. Eng. J.*, 2009, **155**, 886–891.

91 Z. Qin, Q. Yue, Y. Liang, J. Zhang, L. Zhou, O. B. Hidalgo and X. Liu, *J. Biotechnol.*, 2018, **284**, 52–56.

92 M. Kitching, M. Ramani and E. Marsili, *Microb. Biotechnol.*, 2015, **8**, 904–917.

93 J. Guo, M. Suástegui, K. K. Sakimoto, V. M. Moody, G. Xiao, D. G. Nocera and N. S. Joshi, *Science*, 2018, **362**, 813–816.

94 C. T. Dameron, R. N. Reese, R. K. Mehra, A. R. Kortan, P. J. Carroll, M. L. Steigerwald, L. E. Brus and D. R. Winge, *Nature*, 1989, **338**, 596–597.

95 M. Shao, R. Zhang, C. Wang, B. Hu, D. Pang and Z. Xie, *Nano Res.*, 2018, **11**, 2498–2511.

96 R. Cui, H.-H. Liu, H.-Y. Xie, Z.-L. Zhang, Y.-R. Yang, D.-W. Pang, Z.-X. Xie, B.-B. Chen, B. Hu and P. Shen, *Adv. Funct. Mater.*, 2009, **19**, 2359–2364.

97 H. Bao, N. Hao, Y. Yang and D. Zhao, *Nano Res.*, 2010, **3**, 481–489.

98 M. Kowshik, W. Vogel, J. Urban, S. K. Kulkarni and K. M. Paknikar, *Adv. Mater.*, 2002, **14**, 815–818.

99 R. Cui, Y.-P. Gu, Z.-L. Zhang, Z.-X. Xie, Z.-Q. Tian and D.-W. Pang, *J. Mater. Chem.*, 2012, **22**, 3713–3716.

100 Y. P. Gu, R. Cui, Z. L. Zhang, Z. X. Xie and D. W. Pang, *J. Am. Chem. Soc.*, 2012, **134**, 79–82.

101 W. Li, Y. Zhang, Z. Xu, Q. Meng, Z. Fan, S. Ye and G. Zhang, *Angew. Chem.*, 2016, **55**, 955–959.
102 K. Liang, J. J. Richardson, J. Cui, F. Caruso, C. J. Doonan and P. Falcaro, *Adv. Mater.*, 2016, **28**, 7910–7914.
103 K. Liang, J. J. Richardson, C. J. Doonan, X. Mulet, Y. Ju, J. Cui, F. Caruso and P. Falcaro, *Angew. Chem., Int. Ed. Engl.*, 2017, **56**, 8510–8515.
104 W. Geng, N. Jiang, G.-Y. Qing, X. Liu, L. Wang, H. J. Busscher, G. Tian, T. Sun, L.-Y. Wang, Y. Montelongo, C. Janiak, G. Zhang, X.-Y. Yang and B.-L. Su, *ACS Nano*, 2019, **13**, 14459–14467.
105 X. Ma, P. Liu, Y. Tian, G. Zhu, P. Yang, G. Wang and L. Yang, *Nanoscale*, 2018, **10**, 3489–3496.
106 F. Elahian, S. Reiisi, A. Shahidi and S. A. Mirzaei, *Nanomedicine*, 2017, **13**, 853–861.
107 X. Xu, Y. Yang, H. Jin, B. Pang, R. Yang, L. Yan, C. Jiang, D. Shao and J. Shi, *ACS Sustainable Chem. Eng.*, 2020, **8**, 6806–6814.
108 G. Chen, B. Yi, G. Zeng, Q. Niu, M. Yan, A. Chen, J. Du, J. Huang and Q. Zhang, *Colloids Surf., B*, 2014, **117**, 199–205.
109 S. Mirzadeh, E. Darezereshki, F. Bakhtiari, M. H. Fazaelipoor and M. R. Hosseini, *Mater. Sci. Semicond. Process.*, 2013, **16**, 374–378.
110 D. S. Balaji, S. Basavaraja, R. Deshpande, D. B. Mahesh, B. K. Prabhakar and A. Venkataraman, *Colloids Surf., B*, 2009, **68**, 88–92.
111 F. Liu, D. S. Shah and G. M. Gadd, *Curr. Biol.*, 2021, **31**, 358–368.
112 A. Bharde, D. Rautaray, V. Bansal, A. Ahmad, I. Sarkar, S. M. Yusuf, M. Sanyal and M. Sastry, *Small*, 2006, **2**, 135–141.
113 V. Bansal, D. Rautaray, A. Ahmad and M. Sastry, *J. Mater. Chem.*, 2004, **14**, 3303–3305.
114 V. Bansal, D. Rautaray, A. Bharde, K. Ahire, A. Sanyal, A. Ahmad and M. Sastry, *J. Mater. Chem.*, 2005, **15**, 2583–2589.
115 Y. G. Yin, X. Y. Yang, L. G. Hu, Z. Q. Tan, L. X. Zhao, Z. Zhang, J. F. Liu and G. B. Jiang, *Environ. Sci. Technol. Lett.*, 2016, **3**, 160–165.
116 N. Durán, P. D. Marcato, O. L. Alves, G. I. H. D. Souza and E. Esposito, *J. Nanobiotechnol.*, 2005, **3**, 8.
117 A. Mishra, S. K. Tripathy, R. Wahab, S.-H. Jeong, I. Hwang, Y.-B. Yang, Y.-S. Kim, H.-S. Shin and S.-I. Yun, *Appl. Microbiol. Biotechnol.*, 2011, **92**, 617–630.
118 T. Akther, M. Vabeiryureilai, K. Nachimuthu Senthil, M. Davoodbasha and H. Srinivasan, *Environ. Sci. Pollut. Res.*, 2019, **26**, 13649–13657.
119 M. Saravanan, S. Arokiyaraj, T. Lakshmi and A. Pugazhendhi, *Microb. Pathog.*, 2018, **117**, 68–72.
120 G. Rajakumar, A. A. Rahuman, S. M. Roopan, V. G. Khanna, G. Elango, C. Kamaraj, A. A. Zahir and K. Velayutham, *Spectrochim. Acta, Part A*, 2012, **91**, 23–29.
121 X. Liang, M. A. M.-J. Perez, K. C. Nwoko, P. Egbers, J. Feldmann, L. Csetenyi and G. M. Gadd, *Appl. Microbiol. Biotechnol.*, 2019, **103**, 7241–7259.
122 M. Shah, D. Fawcett, S. Sharma, S. K. Tripathy and G. E. J. Poinern, *Materials*, 2015, **8**, 7278–7308.
123 Anshup, J. S. Venkataraman, C. Subramaniam, R. R. Kumar, S. Priya, T. R. S. Kumar, R. V. Omkumar, A. John and T. Pradeep, *Langmuir*, 2005, **21**, 11562–11567.
124 S. Gao, D. Chen, Q. Li, J. Ye, H. Jiang, C. Amatore and X. Wang, *Sci. Rep.*, 2014, **4**, 4384.
125 L. Tan, A. Wan and H. Li, *ACS Appl. Mater. Interfaces*, 2014, **6**, 18–23.
126 L.-H. Xiong, J.-W. Tu, Y.-N. Zhang, L.-L. Yang, R. Cui, Z.-L. Zhang and D.-W. Pang, *Sci. China: Chem.*, 2020, **63**, 448–453.
127 D. Zhang, T. Wu, X. Qin, Q. Qiao, L. Shang, Q. Song, C. Yang and Z. Zhang, *Nano Lett.*, 2019, **19**, 6635–6646.
128 C. Zhao, T. Du, F. U. Rehman, L. Lai, X. Liu, X. Jiang, X. Li, Y. Chen, H. Zhang, Y. Sun, S. Luo, H. Jiang, M. Selke and X. Wang, *Small*, 2016, **12**, 6255–6265.
129 Z. Wei, X. Zhang, T. Yong, N. Bie, G. Zhan, X. Li, Q. Liang, J. Li, J. Yu, G. Huang, Y. Yan, Z. Zhang, B. Zhang, L. Gan, B. Huang and X. Yang, *Nat. Commun.*, 2021, **12**, 440.
130 T. Yong, D. Wang, X. Li, Y. Yan, J. Hu, L. Gan and X. Yang, *J. Controlled Release*, 2020, **322**, 555–565.
131 T. Yong, X. Li, Z. Wei, L. Gan and X. Yang, *J. Controlled Release*, 2020, **328**, 562–574.
132 D. Wang, Y. Yao, J. He, X. Zhong, B. Li, S. Rao, H. Yu, S. He, X. Feng, T. Xu, B. Yang, T. Yong, L. Gan, J. Hu and X. Yang, *Adv. Sci.*, 2020, **7**, 1901293.
133 T. Yong, X. Zhang, N. Bie, H. Zhang, X. Zhang, F. Li, A. Hakeem, J. Hu, L. Gan, H. A. Santos and X. Yang, *Nat. Commun.*, 2019, **10**, 3838.
134 Q. Liang, N. Bie, T. Yong, K. Tang, X. Shi, Z. Wei, H. Jia, X. Zhang, H. Zhao, W. Huang, L. Gan, B. Huang and X. Yang, *Nat. Biomed. Eng.*, 2019, **3**, 729–740.
135 J. Ye, J. Wang, Q. Li, X. Dong, W. Ge, Y. Chen, X. Jiang, H. Liu, H. Jiang and X. Wang, *Biomater. Sci.*, 2016, **4**, 652–660.
136 J. Wang, G. Zhang, Q. Li, H. Jiang, C. Liu, C. Amatore and X. Wang, *Sci. Rep.*, 2013, **3**, 1157.
137 J. Ye, X. Dong, H. Jiang and X. Wang, *J. Mater. Chem. B*, 2017, **5**, 691–696.
138 T. Du, C. Zhao, F. ur Rehman, L. Lai, X. Li, Y. Sun, S. Luo, H. Jiang, M. Selke and X. Wang, *Nano Res.*, 2017, **10**, 2626–2632.
139 S. Shaikh, F. U. Rehman, T. Du, H. Jiang, L. Yin, X. Wang and R. Chai, *ACS Appl. Mater. Interfaces*, 2018, **10**, 26056–26063.
140 L. Lai, C. Zhao, M. Su, X. Li, X. Liu, H. Jiang, C. Amatore and X. Wang, *Biomater. Sci.*, 2016, **4**, 1085–1091.
141 L. Lai, X. Jiang, S. Han, C. Zhao, T. Du, F. U. Rehman, Y. Zheng, X. Li, X. Liu, H. Jiang and X. Wang, *Langmuir*, 2017, **33**, 9018–9024.
142 A. Elfick, G. Rischitor, R. Mouras, A. Azfer, L. Lungaro, M. Uhlarz, T. Herrmannsdoerfer, J. Lucocq, W. Gamal, P. Bagnaninchi, S. Semple and D. M. Salter, *Sci. Rep.*, 2017, **7**, 39755.
143 J. Jin, T. Liu, M. Li, C. Yuan, Y. Liu, J. Tang, Z. Feng, Y. Zhou, F. Yang and N. Gu, *Colloids Surf., B*, 2018, **163**, 385–393.

144 A. Rahman, J. Lin, F. E. Jaramillo, D. A. Bazylinski, C. Jeffryes and S. A. Dahoumane, *Molecules*, 2020, **25**, 3246.
145 E. Rodriguez, J. G. Parsons, J. R. Peralta-Videa, G. Cruz-Jimenez, J. Romero-Gonzalez, B. E. Sanchez-Salcido, G. B. Saupe, M. Duarte-Gardea and J. L. Gardea-Torresdey, *Int. J. Phytorem.*, 2007, **9**, 133–147.
146 L. Marchiol, A. Mattiello, F. Poscic, C. Giordano and R. Musetti, *Nanoscale Res. Lett.*, 2014, **9**, 101.
147 J. L. Gardea-Torresdey, J. G. Parsons, E. Gomez, J. Peralta-Videa, H. E. Troiani, P. Santiago and M. J. Yacaman, *Nano Lett.*, 2002, **2**, 397–401.
148 J. L. Gardea-Torresdey, E. Gomez, J. R. Peralta-Videa, J. G. Parsons, H. Troiani and M. Jose-Yacaman, *Langmuir*, 2003, **19**, 1357–1361.
149 N. C. Sharma, S. V. Sahi, S. Nath, J. G. Parsons, J. L. Gardea-Torresdey and T. Pal, *Environ. Sci. Technol.*, 2007, **41**, 5137–5142.
150 A. Manceau, K. L. Nagy, M. A. Marcus, M. Lanson, N. Geoffroy, T. Jacquet and T. Kirpichtchikova, *Environ. Sci. Technol.*, 2008, **42**, 1766–1772.
151 R. G. Haverkamp, A. T. Marshall and D. van Agterveld, *J. Nanopart. Res.*, 2007, **9**, 697–700.
152 M. Anandan, G. Poorani, P. Boomi, K. Varunkumar, K. Anand, A. A. Chuturgoon, M. Saravanan and H. G. Prabu, *Process Biochem.*, 2019, **80**, 80–88.
153 M. N. Borovaya, A. P. Naumenko, N. A. Matvieieva, Y. B. Blume and A. I. Yemets, *Nanoscale Res. Lett.*, 2014, **9**, 686.
154 P. Prakash, P. Gnanaprakasam, R. Emmanuel, S. Arokiyaraj and M. Saravanan, *Colloids Surf., B*, 2013, **108**, 255–259.
155 A. A. Trofimov, A. A. Pawlicki, N. Borodinov, S. Mandal, T. J. Mathews, M. Hildebrand, M. A. Ziatdinov, K. A. Hausladen, P. K. Urbanowicz, C. A. Steed, A. V. Ievlev, A. Belianinov, J. K. Michener, R. Vasudevan and O. S. Ovchinnikova, *npj Comput. Mater.*, 2019, **5**, 67.
156 N. Kröger, R. Deutzmann and M. Sumper, *Science*, 1999, **286**, 1129–1132.
157 N. Javaheri, R. Dries, A. Burson, L. J. Stal, P. M. A. Sloot and J. A. Kaandorp, *Sci. Rep.*, 2015, **5**, 11652.
158 A. Rahman, S. Kumar, A. Bafana, S. A. Dahoumane and C. Jeffryes, *Molecules*, 2019, **24**, 98.
159 I. Barwal, P. Ranjan, S. Kateriya and S. C. Yadav, *J. Nanobiotechnol.*, 2011, **9**, 56.
160 T. N. V. K. V. Prasad, V. S. R. Kambala and R. Naidu, *J. Appl. Phycol.*, 2013, **25**, 177–182.
161 S. A. Dahoumane, C. Djediat, C. Yepremian, A. Coute, F. Fievet, T. Coradin and R. Brayner, *Biotechnol. Bioeng.*, 2012, **109**, 284–288.
162 D. Parial, H. K. Patra, P. Roychoudhury, A. K. Dasgupta and R. Pal, *J. Appl. Phycol.*, 2012, **24**, 55–60.
163 D. Parial and R. Pal, *J. Appl. Phycol.*, 2015, **27**, 975–984.
164 S. Amar Dahoumane, C. Yepremian, C. Djediat, A. Coute, F. Fievet, T. Coradin and R. Brayner, *J. Nanopart. Res.*, 2016, **18**, 79.
165 S. A. Dahoumane, K. Wijesekera, C. D. M. Filipe and J. D. Brennan, *J. Colloid Interface Sci.*, 2014, **416**, 67–72.
166 Z. Zhang, K. Yan, L. Zhang, Q. Wang, R. Guo, Z. Yan and J. Chen, *J. Hazard. Mater.*, 2019, **374**, 420–427.
167 Z. Zhang, J. Chen, Q. Yang, K. Lan, Z. Yan and J. Chen, *Sens. Actuators, B*, 2018, **263**, 625–633.
168 G. Salas-Herrera, S. Gonzalez-Morales, A. Benavides-Mendoza, A. O. Castaneda-Facio, F. Fernandez-Luqueno and A. Robledo-Olivo, *J. Appl. Phycol.*, 2019, **31**, 2437–2447.
169 R. Brayner, T. Coradin, P. Beaunier, J.-M. Greneche, C. Djediat, C. Yepremian, A. Coute and F. Fievet, *Colloids Surf., B*, 2012, **93**, 20–23.
170 P.-R. Liu, Z.-Y. Yang, Y. Hong and Y.-L. Hou, *Algal Res.*, 2018, **31**, 173–182.
171 K. B. Narayanan and S. S. Han, *Adv. Colloid Interface Sci.*, 2017, **248**, 1–19.
172 M. Alarcón-Correa, J.-P. Günther, J. Troll, V. M. Kadiri, J. Bill, P. Fischer and D. Rothenstein, *ACS Nano*, 2019, **13**, 5810–5815.
173 X. Dong, P. Pan, D.-W. Zheng, P. Bao, X. Zeng and X.-Z. Zhang, *Sci. Adv.*, 2020, **6**, eaba1590.
174 Y. S. Nam, H. Park, A. P. Magyar, D. S. Yun, T. S. Pollom and A. M. Belcher, *Nanoscale*, 2012, **4**, 3405–3409.
175 N.-D. Tam-Triet, Z. Alibay, J. M. Plank, J. E. Cheeney and E. D. Haberer, *ACS Appl. Mater. Interfaces*, 2020, **12**, 126–134.
176 N.-D. Tam-Triet, J. M. Plank, G. Chen, R. E. S. Harrison, D. Morikis, H. Liu and E. D. Haberer, *Nanoscale*, 2018, **10**, 13055–13063.
177 P.-Y. Chen, X. Dang, M. T. Klug, J. Qi, N.-M. Dorval Courchesne, F. J. Burpo, N. Fang, P. T. Hammond and A. M. Belcher, *ACS Nano*, 2013, **7**, 6563–6574.
178 J. C. Zhou, C. M. Soto, M.-S. Chen, M. A. Bruckman, M. H. Moore, E. Barry, B. R. Ratna, P. E. Pehrsson, B. R. Spies and T. S. Confer, *J. Nanobiotechnol.*, 2012, **10**, 18.
179 S.-K. Lee, D. S. Yun and A. M. Belcher, *Biomacromolecules*, 2006, **7**, 14–17.
180 S. Li, M. Dharmarwardana, R. P. Welch, C. E. Benjamin, A. M. Shamir, S. O. Nielsen and J. J. Gassensmith, *ACS Appl. Mater. Interfaces*, 2018, **10**, 18161–18169.
181 O. O. Adigun, G. Novikova, E. L. Retzlaff-Roberts, B. Kim, J. T. Miller, L. S. Loesch-Fries and M. T. Harris, *J. Colloid Interface Sci.*, 2016, **483**, 165–176.
182 K. L. Lee, A. A. Murray, D. H. T. Le, M. R. Sheen, S. Shukla, U. Commandeur, S. Fiering and N. F. Steinmetz, *Nano Lett.*, 2017, **17**, 4019–4028.
183 J. M. Slocik, R. R. Naik, M. O. Stone and D. W. Wright, *J. Mater. Chem.*, 2005, **15**, 749–753.
184 K. I. Alsamhary, *Saudi J. Biol. Sci.*, 2020, **27**, 2185–2191.